8-4-2015 12:00 AM

The Effects of Volatile Fatty Acids on the Performance of Microbial Electrolysis Cells

Nan Yang, *The University of Western Ontario*

Supervisor: Dr. George Nakhla, *The University of Western Ontario*
Co-Supervisor: Dr. Hisham Hafez, *The University of Western Ontario*
A thesis submitted in partial fulfillment of the requirements for the Master of Engineering Science degree in Civil and Environmental Engineering

The Effects of Volatile Fatty Acids on the Performance of Microbial Electrolysis Cells

(Thesis format: Integrated Article)

by

Nan Yang

Graduate Program in Civil and Environmental Engineering

A thesis submitted in partial fulfillment
of the requirements for the degree of
Master in Engineering Science

The School of Graduate and Postdoctoral Studies
The University of Western Ontario
London, Ontario, Canada

Abstract

This study investigated the performance of microbial electrolysis cells (MECs) fed with three common fermentation products: acetate, butyrate, and propionate. Each substrate was fed to the reactor for three consecutive-batch cycles. The results showed high current densities for acetate, but low current densities for butyrate and propionate (maximum values were 6.0 ± 0.28, 2.5 ± 0.06, 1.6 ± 0.14 A/m^2, respectively). Acetate also showed a higher coulombic efficiency of 87 ± 5.7 % compared to 72 ± 2.0 and 51 ± 6.4 % for butyrate and propionate, respectively. This paper also revealed that acetate could be easily oxidized by anode respiring bacteria in MEC, while butyrate and propionate could not be oxidized to the same degree. The utilization rate of the substrates in MEC followed the order: acetate > butyrate > propionate. The ratio of suspended biomass to attached biomass was approximately 1:4 for all the three substrates.

Keywords

Microbial electrolysis cell, volatile fatty acids, hydrogen, biomass

Co-Authorship Statement

Dr. George Nakhla and Dr. Hisham Hafez provided supervision and guidance to the research project.

Chapter 3: Impact of Volatile Fatty Acids on Microbial Electrolysis Cell Performance

Nan Yang, Hisham Hafez, George Nakhla

My contributions are as follows:

- Design and execution of the experimental testing program
- Analysis and interpretation of the findings
- Writing the paper

Subsequent modifications were carried out by Dr. Nakhla and Dr. Hafez.

To my beloved parents for their support,

my boyfriend, Minchao, for his accompany and endless love,

and my nieces, Yunhui and Yunzheng, for their cuteness.

Acknowledgments

I would like to express my deepest appreciation and respect to my advisors' Dr. George Nakhla and Dr. Hisham Hafez for their constant guidance and support. I am deeply touched by Dr. Nakhla's enthusiasm for student training and his way of encouraging his students to think. Dr. Nakhla is very well-known for his continuous-flow strive to maintain high standards and pushing his student to think critically, which was very crucial to develop my potential, and for which I am deeply indebted. Without his encouragement and pushes, I could not have achieved the utmost of my potential. Dr. Hisham Hafez also offered me a lot of help throughout my master studies. I am grateful for his kindness and support.

I would like to express my sincere gratitude to Dr. Elsayed Elbeshbishy and Bipro Dhar for their help during the start-up of the reactors. I would also like to thank my colleague and good friends, especially Medhvi Gupta, Noha Nasr, Maritza Gomez-Flores, Chinaza Akobi, Basem Haroun, Joseph Donohue, Nael Yasri, Zhenqi Wang, Kai Li, Xiaoguang Liu, Mingu Kim, Manoli Kyriakos. They are always so kind, helpful, and cheerful. I feel very lucky to be one of this wonderful team. Last but not least, I would like to thank my family, my boyfriend, and my friends, for their priceless care, inspiration, and endless love.

Table of Contents

List of Tables

List of Figures

Nomenclature

ABR	Anaerobic baffled reactor
AEM	Anion exchange membrane
ARB	Anode respiring bacteria
BEAMR	Bio-electrochemically assisted microbial reactor
BES	Bioelectrochemcial system
CEM	Cation exchange membrane
COD	Chemical oxygen demand
DPRB	Dissimilatory perchlorate reducing bacteria
EET	Extracellular electron transfer
HER	Hydrogen evolution reaction
HRT	Hydraulic retention time
MECs	Microbial electrolysis cells
MFCs	Microbial fuel cells
PEM	Proton exchange membrane
SCOD	Soluble chemical oxygen demand
SRB	Sulfate reducing bacteria
UASB	Up-flow anaerobic sludge bed
UBER	Up-flow biocatalyzed electrolysis reactor
VFAs	Volatile fatty acids

Chapter 1

Introduction

1.1 Background

Hydrogen potentially plays a key role in sustainable energy production. It can be recovered by dark fermentation of organic material rich in carbohydrates, but a major fraction of organic matter remains in the form of volatile fatty acids (VFAs) (Liu et al., 2005).

Theoretically, 12 moles of hydrogen can be extracted from 1 mole of glucose, if the complete conversion reaction to hydrogen is taken into account (Eq. (1)). However, in practice, only less than 33% of the theoretical hydrogen production can be achieved, since part of the original substrate remains as acetate (Eq. (2)) and some of the organic matter is used for biomass synthesis. Moreover, organic intermediates also act as electron scavengers, which lead to the production of other fermentation products such as propionate, butyrate, lactate, formate and alcohols. In case the butyrate fermentation pathway is established, the conversion efficiency is reduced to 2 mol H_2/mol glucose (Eq. (3)) (Gioannis et al., 2013). Further utilization of these volatile fatty acids to produce more hydrogen is very promising.

$$C_6H_{12}O_6 + 6H_2O \rightarrow 12H_2 + 6CO_2 \quad (1)$$

$$C_6H_{12}O_6 + 2H_2O \rightarrow 4H_2 + 2CO_2 + 2CH_3COOH \quad (2)$$

$$C_6H_{12}O_6 \rightarrow 2H_2 + 2CO_2 + CH_3CH_2CH_2OOH \quad (3)$$

To achieve a higher conversion of a substrate to hydrogen, an addition to fermentation to achieve a higher hydrogen yield is the process of electrohydrogenesis using microbial electrolysis cells (MECs).

Recently, combining dark fermentation with MECs seems to be very promising. Some researches use dark fermentation effluent as the MEC influent or combine dark fermentation with MEC/MFC together. As the main end products from dark fermentation, VFAs have a vital impact on the performance of MECs. Currently, most MECs use acetate as the benchmark substrate Acetate and butyrate proved to be easily degradable, whereas propionate exhibited pseudo-recalcitrant behavior in a continuous-flow two-chamber MEC (Escapa et al., 2013).

In this study, a two chamber microbial electrolysis cell (MEC) was used to oxidize acetate, butyrate and propionate individually, and the effects of different substrates on the performance of MEC were assessed.

1.2 Research Objectives

The main goal of this study was to further explore the use of dark fermentation effluent comprising VFA mixtures in MECs. The specific objectives are as follows:

- To clear the contradiction in the literature regarding the relative biodegradability of butyrate and propionate in MECs.
- To further explore the use of dark fermentation effluent in MECs.
- To assess the impact of VFAs on MEC performance.
- To establish the relationship between attached biomass and suspended biomass for butyrate and propionate in MEC.
- To compare the impact of initial concentration of chemical oxygen demand (COD) on the performance of MECs

1.3 Research Contributions

Even though a handful of literature studies investigated the performance of MECs with different VFAs, there is a contradiction in the literature regarding the relative biodegradability of butyrate and propionate in MECs. In this research, a comprehensive comparison of the effects of acetate, butyrate, and propionate on MEC is undertaken. Furthermore, for the first time the relationship between attached biomass and suspended biomass for butyrate and propionate in MEC has been established.

1.4 Thesis Organization

This thesis includes four chapters and two appendices, which confirm to the "integrated article" format as outlined in the Thesis Regulation Guide by the School of Graduate and Postdoctoral Studies (SGPS) of the University of Western Ontario. The thesis consists of the following chapters:

Chapter 1 -- presents the general background, research objectives, and research contributions

Chapter 2 – presents a literature review on MEC materials, configurations, and performances

Chapter 3 – discusses the effects of different VFAs on the performance of MEC

Chapter 4 – recommendations for future work based on the literature review and the results of this study

1.5 References

1. Escapa, A., Lobato, A., García, D., Morán, A. 2013. Hydrogen production and COD elimination rate in a continuous-flow microbial electrolysis cell: The influence of hydraulic retention time and applied voltage. Environ. Prog. Sustain. Energy. 32, 263-268.

2. Gioannis, G.D., Muntoni, A., Polettini. R.P. 2013. A review of dark fermentative hydrogen production from biodegradable municipal waste fractions. Waste Management. 33, 1345-1361.

3. Logan, B.E., Call, D., Cheng, S., 2008. Microbial electrolysis cells for high yield hydrogen gas production from organic matter. Environ. Sci. Technol. 42,23-8631.

4. Liu, H., Cheng, S., Logan, B.E. 2005. Production of electricity from acetate or butyrate using a single-chamber microbial fuel cell. Environ. Sci. Technol. 39, 658-662.

Chapter 2

Literature Review

2.1 Introduction

In recent years, bioelectrocatalysis using microorganisms as catalysts for bioelectrochemcial system (BES) has become very promising for wastewater treatment and removal of various contaminants via electrobiochemical reactions (Wang et al., 2012). In a BES, organic compounds such as acetate, glucose, volatile fatty acids, protein, domestic wastewater, etc. and inorganic compounds such as sulfide (Rabaey et al., 2006) are oxidized at the anode. At the cathode, reduction of oxygen or other electron acceptors such as nitrate, nitrobenzene, perchlorate, sulfate occurs. The bioanode, at which microorganisms convert the chemical energy in organic matter to electrical energy, forms the basis of most BESs (Sleutels et al., 2013). These systems are referred to as Microbial Fuel Cells (MFCs) when electricity is produced or Microbial Electrolysis Cells (MECs) when electrical energy is added to the chamber.

In MFCs, bacteria growing on the anode, oxidize organic matter and release carbon dioxide and protons into solution and electrons to the anode. The cathode is sparged with air to provide dissolved oxygen for the reactions of electrons, protons and oxygen at the cathode, with a wire (and load) to complete the circuit and produce power (Logan, 2008a).

When oxygen is present at the cathode, current can be produced, but without oxygen, current generation is not spontaneous. However, when applying a voltage (>0.2V in theory) to the system, hydrogen gas is produced at the cathode through the reduction of protons (Logan et al., 2008b). In MECs, the anode-respiring bacteria (ARB), such as *Geobacter Shewanella*, *Pseudomonas*, *Clostridium*, *Desulfuromonas*, *Esehericha*, and *Klebisella*, are attached to the

conductive anode where they oxidize organic compounds and transfer the electrons through an external electrical circuit to the cathode (Lee et al., 2010). The electrons reach the cathode and react with water to produce H_2. This system has previously been named as bio-electrochemically assisted microbial reactor (BEAMR) or a biocatalyzed electrolysis cell. Because the standard potential of the organics (e.g. $E_{acetate}$ = -0.28 V) is more positive than for H_2 (E_{H2} = -0.41 V), and also due to energy losses, electric power supply must be added into the reactor. The typical range of applied voltage is 0.6 V to 1.2 V (Logan, 2008a).

To date, MECs as a new technology to produce bio-fuels and degrade wastewater have been extensively reviewed. These include a brief overview of recent advances in research on electrochemically active bacteria, MEC materials and design, as well as a critical review of high hydrogen yield from various feedstock (Liu et al., 2010), an overview of cathode material and catalysts suitable for generating hydrogen in microbial electrolysis cell (Kundu et al., 2013), and a review of the substrates used in microbial electrolysis cells (MECs) for producing sustainable and clean hydrogen gas (Kadier et al., 2014).

However, a comprehensive review of research on continuous-flow MEC, which is very important for scaling up, is still lacking. The development of continuous-flow MECs during the past years based on the number of journal papers being published is shown in Figure 2.1. The number of continuous-flow papers was very low before the year of 2008. The continuous-flow studies increased from 19 in 2008 to 48 in 2014. The ratio of continuous-flow to total papers published on MECs also increased with time, from 33% in 2006 to 52% in 2014. Furthermore the modification of MECs for continuous-flow wastewater treatment, their advantages and challenges have been explored.

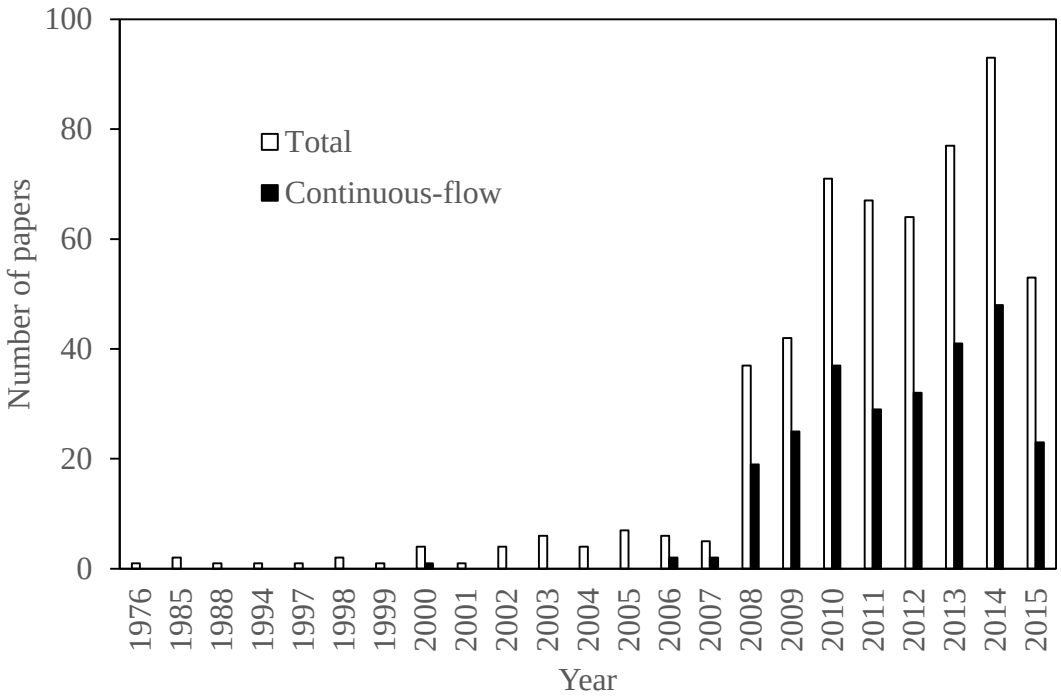

Figure 2.1 –The development of continuous-flow MECs during the past years based on the number of journal papers being published. The total number of articles is based on "Scopus" search using "microbial electrolysis cell" as key word in July 2015, while the number of continuous-flow articles is further limited to "continuous" as refined key word.

2.2 Materials

2.2.1 Anode

Almost all the research in MECs has utilized carbon-based materials for the anode, except for bio-cathode MECs because the microorganisms are grown on the cathode instead of anode. The carbon-based anodes are so popular because of their good conductivity, biocompatibility, low over-potentials and relatively low cost (Logan et al., 2008).

Common materials in laboratory scale MECs operated in continuous-flow mode include carbon felt (Sleutels et al., 2013; Tartakovsky et al., 2009), carbon mesh (Cusick et al., 2014), carbon brush (Cui et al., 2012; Wang et al., 2012), carbon fiber (Dhar et al., 2013), graphite felt

(Jeremiasse et al., 2010), graphite granules (Gusseme et al., 2012), graphite powder (Thrash et al., 2007) and graphite fiber (Lee & Rittmann, 2009).

Ammonium treatment of carbon electrodes have become a widely applicable method for increasing the performance of both MFCs and MECs by facilitating the attachment of microorganism and increasing electron transfer to the anode surface area (Cheng & Logan, 2007). Optimal heat treatment in the laboratory for the brush anodes was reported as 450°C for 30 min (Wang et al., 2009). The advantages of this treatment are: (1) to a faster start-up, (2) higher current densities. The aforementioned advantages are attributed to the more favorable adhesion of microorganisms to the positively charged anode and to improved electron transfer to the chemically modified surface (Cheng et al., 2007). However, at full-scale, the cost of heat pre-treatment appears be a challenge.

Wang et al. (2010) have demonstrated that the electricity output and conversion of acetate to hydrogen were increased with a packed bed of graphite granules as electrodes. A graphite rod was inserted in the bed as a current collector. Titanium or stainless steel is always served as the current collector when the carbon materials are in fiber or brush form.

Porous electrodes such as graphite felt also have the potential to generate higher volumetric current densities due to the high specific surface area. Sleutels et al. (2009) studied the effect of mass and charge transport on current densities using three thicknesses (1, 3, 6.5 mm) of graphite felt anode. A spacer material (64% open; PETEX 07-4000/64, Sefar BV, Goor, The Netherlands) with a total thickness of 4 mm was placed between the anode and the membrane, so that the anolyte was forced to flow perpendicular to the felt. The aforementioned researchers found that without the flow force, i.e., when the flow is parallel to the anode, the thicker the graphite, the lower is the

current density. This was because in thicker types of felt the substrate was limiting microbial growth in deeper parts of the felts. With the forced flow, this system reached a high current density of 16.4 A m^{-2} and a hydrogen production rate of 5.6 m^3 m^{-3} d^{-1} at an applied voltage of 1 V with a 50 mM phosphate buffer solution. This research showed that the current densities in porous electrodes can be improved by the force flow of anolyte through the electrode.

2.2.2 Cathode

Most of the cathode material used in continuous-flow MEC systems are stainless steel mesh (Dennis et al., 2013; Nam et al., 2014), platinum (Pt) coated with titanium (Sleutels et al., 2013), nickel (Ni) foam (Jeremiasse et al., 2010), carbon paper or carbon cloth coated with Pt or Ni (Hrapovic et al., 2010), and graphite granules (Gusseme et al., 2012). When it comes to biocathodes, carbon materials are always used as the cathode.

Unlike anode materials, plain carbon materials are rarely used as cathode since the hydrogen evolution reaction (HER) on plain carbon electrodes is very slow, requiring a high overpotential (-0.42 V at pH 7) to drive hydrogen production (Rozendal et al., 2007; Logan et al., 2008).

It has been shown in the literature that adding specific chemicals to highly conductive surfaces can greatly affect electron transfer. Hrapovic et al. (2010) developed a low cost MEC cathode by Ni electrodeposition onto a porous carbon paper, and evaluated different Ni or Pt loadings. The aforementioned authors found that at a Ni load of 0.2-0.4 mg cm^{-2} under acetate non-limiting conditions, hydrogen production could reach 5.4 L L^{-1} d^{-1} with a corresponding current density of 5.7 A m^{-2}. This hydrogen production rate was significantly greater than the volumetric rate of 2.0-2.3 L L^{-1} d^{-1} reported for a batch-operated MEC quipped with similar anodes

and Ni alloy or NiW cathodes (Hu et al., 2009). According to the authors, the improved rate of hydrogen production was due to an optimized Ni load and the high porosity of the gas diffusion cathodes, which provided a higher surface area for Ni electrodeposition, compared to the solid metal sheets used by Selembo et al (2009). Moreover, this study proved that Ni is a better catalyst than Pt in MECs. Manuel et al. (2010) studied the impact of the catalyst load on hydrogen production rate, and concluded that the chemical deposition of Ni can be successfully employed for continuous-flow production of hydrogen in a MEC.

Instead of using Ni as a deposited catalyst onto carbonaceous materials, Jeremiassa et al. (2010) investigated the nickel as the cathode, because of its low electrical resistivity, availability, stability in highly alkaline solutions, low price, and reported a hydrogen production as high as 50 $m^3\ m^{-3}\ d^{-1}$ and a current density of 22.8 ± 0.1 A m^{-2} with electrical energy input of 2.6 KWh m^{-3} H_2.

Despite its success in fed-batch MEC and MFC studies, stainless steel have not been studied in continuous-flow studies.

2.2.3 Membrane

A membrane can be used to separate the chamber where microorganisms degrade the substrate from the one where hydrogen evolves (Logan et al., 2008). The advantages of applying the membrane are minimization of hydrogen losses by anodic bacteria and in the liquid, and prevention of hydrogen gas from mixing with carbon dioxide in the anode, while its disadvantages are the increase in potential losses associated with the membrane, and the reduction of energy recovery.

Cation exchange membranes (CEMs) have been used in several studies with limited success since cations, such as Na^+, K^+, NH_4^+, Ca^{2+} and Mg^2, can be transported more efficiently than protons through the membrane (Rozendal et al., 2006; Zhao et al., 2006). The reason is that the pH of the substrate in MEC is close to 7, which means only about 10^{-4} mM of protons are present in the anode chamber, orders of magnitude lower than the typical cations concentrations (Rodendal et al., 2007).

If H^+ cannot be effectively transported across a CEM, then the pH cannot be effectively balanced in an MEC. A possible solution to the pH gradient associated potential losses is the application of an anion exchange membrane (AEM) instead of a CEM. Rozend et al. (2007) discovered that the AEM is better capable of preventing the pH gradient across the membrane than the CEM (CEM ΔpH = 6.4; AEM ΔpH = 4.4). Consequently, the pH gradient associated potential losses were lower in the AEM configuration (CEM 0.38V; AEM 0.26 V). Sleutels et al. (2013) also made a comparison between AEM and CEM configurations, as shown in Table 2.1. At steady-state operation, a current density of 10.2 A m^{-1} (909 A m^{-3}) at an applied voltage of 1.0 V was produced in the AEM, compared to 7.2 A m^{-2} (643 A m^{-3}) for the CEM (Sleutels et al., 2013). The difference between the current densities was due to the lower resistance for transport of ions through the membrane for the AEM configuration compared to the CEM configuration (Sleutels et al., 2013).

There are two theories for the proton transfer mechanism in the literature. Logan et al. (2008a) found that an AEM can allow proton conduction via negatively charged species such as phosphate anions that can be added at high concentration. However, on the other hand, Rozendal et al. (2007) discovered that in an AEM, electroneutrality is achieved by the transport of anions from the cathode to the anode. For biocatalyzed electrolysis this implies that hydrogen at the

cathode is not produced from the reduction of protons, but from the reduction of water that diffuses through the membrane from the anode to the cathode (Rozendal et al., 2007).The two aforementioned transfer mechanisms are depicted in Figure 2.2.

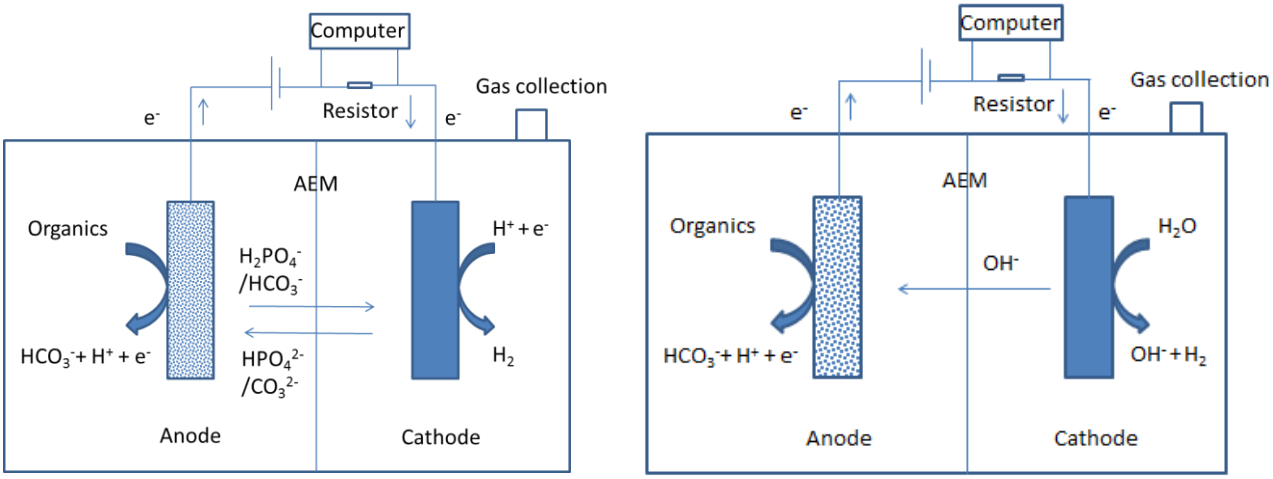

Figure 2.2 – Proton transfers from anode to cathode by negative charges through AEM (left) and hydroxide transfers from cathode to anode through AEM (right).

In order to study the effect of membrane on MEC performances, Tartakovsky et al. (2009) constructed two gas-phase cathode MECs operating in continuous-flow mode, one with a proton exchange membrane (PEM, Nafion 117), and the other without membrane. The absence of PEM reduced the internal resistance form 27 Ω to 19 Ω. At an acetate loading rate of 4 g L_A^{-1} d^{-1} (i.e., 4 g per day per liter of anode), hydrogen production rates of 1.0-1.3 L_{STP} $L_A^{-1}d^{-1}$, and 6.1-6.5 L_{STP} $L_A^{-1}d^{-1}$ were obtained in MEC with membrane and MEC without membrane, respectively. These values are comparable with the hydrogen production rate of 1 L $L_A^{-1}d^{-1}$ observed in a MEC equipped with a PEM (Rozendal et al., 2007) and a rate of 3 L $L_A^{-1}d^{-1}$ observed in a single chamber membrane-free MEC (Call & Logan, 2008b). Single-chamber membrane-free MECs were designed by Hu et al. (2008) and successfully produced hydrogen from organic matter using one

mixed culture (using local domestic wastewater as the inoculum) and one pure culture (*Shewanella oneidensis* MR-1). At an applied voltage of 0.6V, this system with a mixed culture achieved a hydrogen production rate of 0.53 m^3 day^{-1} m^{-3} with a current density of 9.3 A m^{-2} at neutral pH and 0.69 m^3 d^{-1} m^{-3} with a current density of 14 A m^{-2} at pH 5.8 (Hu et al., 2008). The current hydrogen production rates in the pure culture system were much lower than those with mixed culture systems. The performance of single chamber MECs under continuous-flow mode is shown in Table 2.2.

Lee et al. (2009) found that the longer the hydraulic retention time (HRT), the higher the COD removal efficiency, but that corresponded to a lower current density. This illustrated that the feeding mode, either batch or continuous mode, has a big impact on the performance of MECs. The higher hydraulic retention time leads to a lower organic loading rate. The following equations depict the relationship between organic loading rate and current density.

$$1\ mol\ e^- = 8\ g\ COD \quad (1)$$

$$1\ mol\ e^- = 96485\ C \quad (2)$$

$$Organic\ loading\ rate\ (OLR) = \frac{g\ COD}{m^3 d} = \frac{1 mol\ e^-}{8\ m^3 d} = \frac{96485\ C}{8 m^3 86400 s} = 0.14\ \frac{A}{m^3} \quad (3)$$

From equations (1) and (2), the relationship between organic loading rate and current density in continuous-flow MEC could be derived. Equation (3) illustrates that the organic loading rate is proportional to the current density in an MEC. Even though, in practice, there are other factors that can affect the aforementioned ratio of OLR to current density, generally higher organic loading rates, translate to higher current densities. In a single chamber MEC, the current density

decreased from 1630 to 1470 A m^{-3}, when the organic loading rate decreased from 16.3 to 4.02 g COD $L^{-1}d^{-1}$ (Lee et al., 2009).

Operating MECs in continuous-flow mode has become increasingly popular since 2008, because it can achieve better performance than batch MECs. For example, hydrogen production rate was 5.4 L d^{-1} L^{-1} under acetate non-limiting conditions in a Ni cathode MEC operating in continuous-flow mode, compared to 2.3 L d^{-1} L^{-1} under batch mode operation (Hrapovic et al., 2010). Moreover, coulombic efficiency increased from 45% to 86% upon changing the operational mode from batch to continuous-flow in a dual-chamber H-type MEC (Torres el al., 2007). Villano et al. (2012) also demonstrated a remarkable increase in current generation from 18 mA to 120 mA when the MEC was switched from batch to continuous-flow mode. The aforementioned studies suggest that the feeding regime has a big impact on the MEC performance.

In a batch mode MEC, the substrate is added at the beginning of each cycle, and the MEC is fed when the current density drops significantly. Thus in batch mode, the ARBs are operating at viable substrate concentrations, which at times could be limiting growth. However in the continuous-flow mode MEC, the soluble COD fed into the reactor can be controlled by the hydraulic retention time, or organic loading rate, which lead to a non-substrate limiting condition and achieve a better performance.

Table 2.1 -- Design and performance of two-chamber MECs in continuous-flow mode

Anode Material	Cathode Material	Anolyte	V_{an} (mL)	V_{cat} (mL)	Membrane	Eap (V) (unless otherwise stated)	Operation	I_A (A/m^3)	Ref.
Graphite fiber brush	Stainless steel mesh (type 304 SS #60 mesh) coated with platinum	Synthetic wastewater (sodium acetate 1.5 g/L) 1.17 g COD/L*	137	137	AEM	0.9	HRT=1 day OLR = 1.17 g COD/L/d	112*	(Nam et al., 2014)
		Cellulosic fermentation wastewater (FWW) (VFAs+alchohols+proteins) produced by *Clostridium sp.* (1.256 g COD/L)					OLR = 1.256 g COD/L/d	99*	
Carbon felt	platinum coated (50 g/m^2) titanium mesh (1mm thickness)	Sythetic wastewater (1.36 g/L $NaCH_3COO•3H_2O$), 0.64 g COD/L *	280	280	CEM	0.6	HRT = 0.9 h, flow rate: 5 mL/min, OLR = 17 g COD/L/d*	85*	(Sleutels et al., 2013)
						0.8		245*	
						1		643*	
					AEM	0.6		100*	
						0.8		429*	
						1		909*	
Graphite granules	Graphite granules (diameter between 2 and 6 mm), porosity of 0.48	Acetate (0.64 g COD/L)	860	860	PEM	Anode potential at +2.00V (vs. SHE)	Anode flow rate 1.44 L/d, HRT = 14.33 h, OLR = 1.08 g COD/ L/d	116 *	(Villano et al., 2012)

Table 2.1 – (Continued) Design and performance of two-chamber MECs in continuous-flow mode

Anode Material	Cathode Material	Anolyte	V_{an} (mL)	V_{cat} (mL)	Membrane	Eap (V) (unless otherwise stated)	Operation	I_A (A/m^3) (	Ref.
Graphite felt	Ni foam (10 × 10 × 0.2 cm, 1360 kg/m3) (128 m2/m2 projected area)	2.72 g/L $NaCH_3COO{\cdot}3H_2O$ (1.07 g COD/L*)	20 *	20 *	AEM	1	Flow rate: 1.3 mL/min; HRT = 0.26 h*; OLR = 99 g COD/L/d*	5704±32	(Jeremiasse et al., 2010)
Graphite felt (1 mm)	platinum coated (50 g/m2) titanium mesh (projected surface area 0.025 m2)	Synthetic wastewater (1.36 g/L $NaCH_3COO{\cdot}3H_2O$) (0.64 g COD/L*)Rate: 5 mL/min; HRT = 0.039 d*; OLR = 16.46 g COD/L/d*	280	280	AEM	1	No force flow	582	(Sleutels et al., 2009)
Graphite felt (3 mm)							No force flow	438	
Graphite felt (6.5 mm)							No force flow	453	
Graphite felt (1 mm)							With force flow	732	
Graphite felt (3 mm)							With force flow	641	
Graphite felt (6.5 mm)							With force flow	607	

* refers that the data are calculated based on the information from the literature.

Table 2.2 -- Design and performance of single chamber MECs in continuous-flow mode

Anode Material	Cathode Material	Substrate	V (mL)	Eap (V) (unless otherwise stated)	Operation	Current density (A/m^2) (unless otherwise stated)	COD Removal (%) (unless otherwise stated)	Coulombic Efficiency (%)	H2 Production Rate (m^3H_2/m^3d)	H_2 Yield (mol/mol) (unless otherwise stated)	I_A (A/m^3)	Ref.
8 ammonia treated graphite brushes	stainless steel 304 mesh sheet	1 g/L Acetic acid; HRT = 1 day, flowrate = 1.67 mL/min	2400	0.9		1.18	31-47	on day 3: 147; on day 8: 102; on day 18: 135	0.53		71	(Rader & Logan, 2010)
three bundles of graphite fiber	one bundle of graphite fiber	17 mM acetate, HRT from 6.5 to 1.6 h	125	Anode potential -0.126 V (vs SHE)	6.5 h 3.1 h 1.6 h		83 61 37		2.64±0.01 3.70±0.03 4.32±0.46	2.03±0.07 1.88 1.81±0.19	1470 1590 1630	(Lee & Rittmann, 2009)
heat treated graphite brush	carbon cloth with 0.5 mg/cm^2 Pt	1.5 g/L; 50 mM PBS, pH=7.04,	28	0-0.2 V (vs. Ag/AgCl)		147 ±12 A/m3	90± 6	81 ±9	1.2 ± 0.4			(Nam et al., 2011)

2.3 Microorganisms

Most forms of respiration involve a soluble compound (e.g. oxygen, nitrate, and sulfate) as an electron acceptor; nevertheless, some microorganisms are able to respire solid electron acceptors (metal oxides, carbon, and metal electrodes) in order to obtain energy (Torres et al., 2009). Extracellular electron transfer (EET), which refers to electron transport to the surface of the solid electron acceptor, is now the most acceptable explanation of how microorganisms respire using a solid electron acceptor. Researchers have discovered three distinct EET mechanisms, which are shown in Figure 2.3. The first mechanism presents direct electron transfer between electron carriers in the bacteria and the solid electron acceptor (Torres et al., 2009). The second mechanism occurs in the presence of a soluble electron shuttle, which is a compound (e.g. melanin, phenazines, flavins, and quinones) that carries electrons between the bacteria and the electrode by diffusive transport (Newman & Kolter,, 2000; Turick et al.,2002; Hernandez et al., 2004; von Canstein et al., 2008). The third mechanism proposes a solid component (cellular pili as nanowires) that is part of the extracellular biofilm matrix and is conductive for electron transfer from the bacteria to the solid surface (Reguera et al., 2005; Gorby et al., 2006).

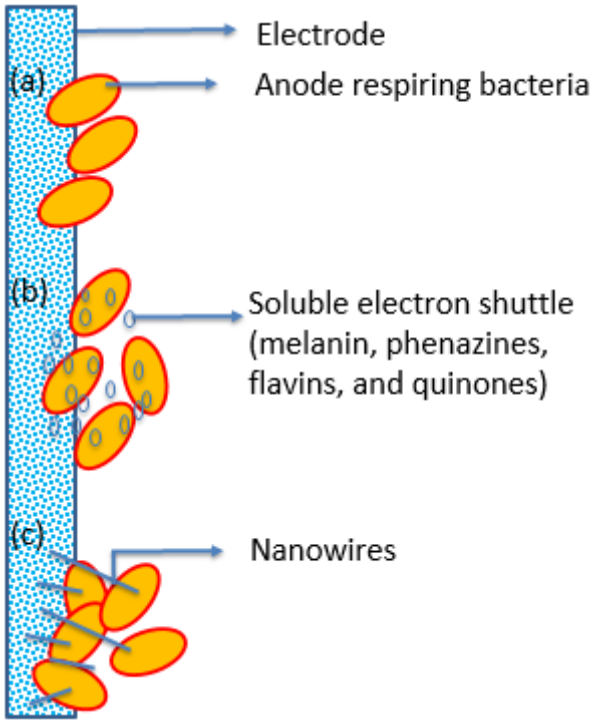

Figure 2.3 – Schematic of three EET mechanisms used by ARB: (a) direct electron transfer, (b) soluble electron shuttle, and (c) cellular pili as nanowires.

Liu et al. (2008) studied the community analysis of an MEC and observed that *Pseudomonas spp*. and *Shewanella spp.* existed on the anode. However, because MECs operate under completely anaerobic conditions, both the obligate anaerobic bacteria, such as exoelectrogenic *Geobacter spp*., and nonexoelectrogenic fermentative (or methanogenic microorganisms) are promoted.

Usually, researchers enrich the bacterial community for a working MFC. The advantages of this procedure are: (1) ensuring biofilm formation on the anode, (2) preselecting an exoelectrogenic community for MECs operation. Moreover, the biofilm can be scraped from the anode and transferred to a new electrode. Last but not least, the effluent from an MFC/MEC

containing exoelectrogenic community (presumably displaced from the anode) can be used as an inoculum.

Methanogenesis could be a problem in MECs, because high concentrations of hydrogen gas favors the growth of hydrogenotrophic methanogens, which reduces hydrogen gas production and contaminates the gas with methane. Three methods can be applied to suppress the growth of methanogens, including: (1) lowering the environment pH by using a medium solution (pH 5.8) containing phosphate buffer, (2) exposing the cathode to air for 15 min when the methane content in the headspace was higher than 5%, (3) boiling the anodes from MFCs for 15 min before placing them in MECs (Hu et al., 2008).

2.4 Modification of MEC design

2.4.1 Multi-electrode

In order to examine the scalability of a multi-electrode MEC, Rader et al (2010) constructed a 2.5 L single chamber MEC containing 8 separate electrode pairs made of graphite fiber brush anodes pre-acclimated in MFC using acetate, and 304 stainless steel mesh cathodes (64 m^2 m^{-3}) under continuous-flow conditions, as shown in Figure 2.4. A voltage of 0.9 V was applied across each pair of electrodes using four separate power supplies. The liquid volume was controlled at ~ 2.4 L to allow a headspace in the reactor for collection and analysis in the tubes. The MEC was operated with a continuous-flow substrate flow at a flowrate of 1.67 mL min^{-1}, a hydraulic retention time (HRT) of 1 day, with acetic acid concentration of 1 g L^{-1}. The maximum current was 181 mA (1.18 A m^{-2} cathode surface area; 74 A m^{-3}) with a maximum hydrogen production of 0.53 L L^{-1} d^{-1} in three days of operation. Current production remained almost steady (days 3-18), but the gas composition dramatically shifted over time. The methane production increased from 0.049 L L^{-1} d^{-1} (day 3) to 0.118 L L^{-1} d^{-1} (day 16). The energy efficiency relative to electrical energy input

remained above 100% until day 17, with a maximum energy efficiency of 144% on day 3.

The maximum observed current density in the aforementioned study of 1.18 A m^{-2} is lower than the current density achieved by Selembo et al (2009), of 4.6 A m^{-2}, despite the use of the similar electrode architecture due to two reasons: namely the use of plastic separators between the electrodes, which may have inhibited proton diffusion from the anode to cathode, and a larger electrode spacing.

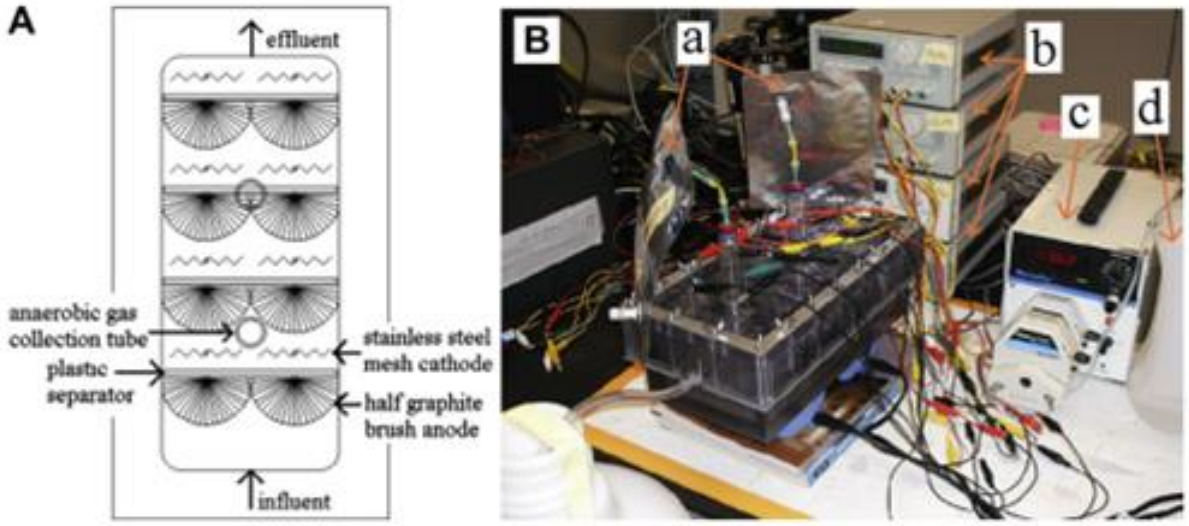

Figure 2.4 – (A) Schematic (top view) and (B) photograph of the 2.5 L scale-up continuous-flow microbial electrolysis cell containing 8 half graphite brush anodes and 8 stainless steel mesh cathodes: (a) gas bag, (b) power sources, (c) fluid pump, and (d) substrate feed tank. (Rader et al., 2010)

3.4.2 Gas-phase Cathodes

Tartakovsky et al (2009) developed a membrane-less continuous-flow microbial electrolysis cell with a gas-collection cathode, as shown in Figure 2.5. This MEC was constructed of a carbon felt anode and a gas diffusion cathode with a Pt loading of 0.5 mg cm^{-2}. The anode and cathode were 0.3 mm apart, separated by a piece of J-cloth. The aforementioned authors compared

the performance of the MEC with a proton exchange membrane (PEM) and without PEM, and also examined the effect of voltage on hydrogen production. The absence of PEM reduced the internal resistance from 27 Ω to 19 Ω. At an acetate loading rate of 4 g L_A^{-1} d^{-1}, hydrogen production rates of 1.0-1.3 L_{STP} $L_A^{-1}d^{-1}$, and 6.1-6.5 L_{STP} $L_A^{-1}d^{-1}$ were obtained in MEC with membrane and MEC without membrane, respectively. These values are comparable with hydrogen production rate of 1 L $L_A^{-1}d^{-1}$ observed in a MEC equipped with a PEM (Rozendal et al., 2007) and a rate of 3 L $L_A^{-1}d^{-1}$ observed in a single chamber membrane-free MEC (Call & Logan, 2008). Hydrogen production rate increased in response to the increase in voltage, at applied voltage between 0.4 and 1.0 V. At an applied voltage of 1 V, a power input of 2 Wh L^{-1}-H_2, a hydrogen yield of 3.9 mol mol^{-1}-acetic acid, and a current density of 4.7 A m^{-2} was achieved.

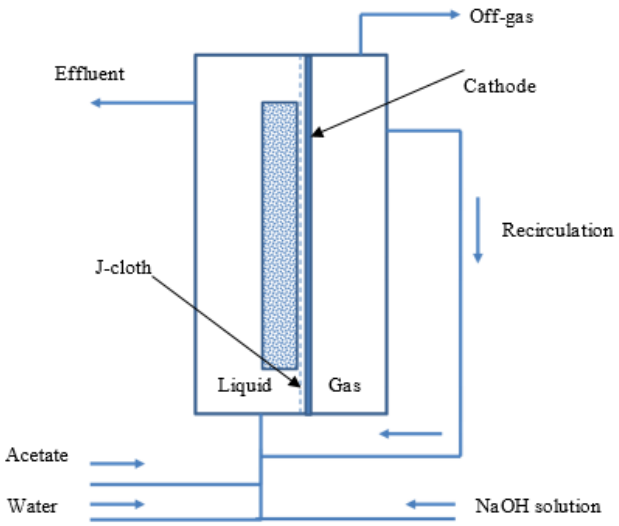

Figure 2.5 – Diagram of a continuous-flow MEC setup. (Modified from Tartakovsky et al., 2009)

This MEC design was also used by Escapa et al. (2012) to test the effect of organic loading rate and applied voltage on hydrogen production rates when treating full-strength domestic

wastewater, as shown in Table 2.3. A graphite felt anode and a Ni-based gas diffusion cathode with a Ni load of 0.4 mg cm^{-2} cathode were used. J-cloth with a thickness of 0.7 mm was also used in this MEC. At an organic loading rate of 441 mg L_A^{-1} d^{-1} and applied voltage of 0.75 V, a maximum of COD reduction of 76% was achieved in this reactor. H_2 only evolved at organic loading rates between 448 mg L_A^{-1} d^{-1} and 1994 mg L_A^{-1} d^{-1} at an applied voltage of 1 V. Hydrogen production rate as a function of the organic loading rate fit a Monod-type model, with a maximum hydrogen production constant of 0.462 L L_A^{-1} d^{-1} and a half saturation coefficient of 1342 mg L_A^{-1} d^{-1}, and proved to be highly dependent on the influent COD.

The main advantage of this design is that hydrogen produced in the liquid chamber can be directly released to the gas collection chamber due to lower mass transfer resistance compared with the gas transfer through a liquid phase. The challenges of this design could be the cathode leaking or flooding, and due to the absence of membranes, hydrogen could easily crossover from the cathode to the anode leading to significant hydrogen re-oxidation.

Table 2.3 Design and performance of MEC with gas-phase cathode in continuous-flow mode

System Description			System Performances								
Anode	Carbon Cloth Based Gas Diffusion Cathode(GDC)/metal mg/cm2	Carbon Source	Eap (V)	I_A (A/m2)	Q_{H2} (L/ L/d)	Y_{H2} (mol/mol)	Win (Wh/ L)	η_{COD} (%)	CE (%)	η_E (%)	Ref.
Carbon felt	GDC/0.5 Pt	Sodium acetate: 90.7 g/L, Acetate load of 4.0 g/L/d (pump rate: acetate solution: 5.0 mL/d, trace metals dilution solution: 140 mL/d; HRT=10 h)	0.4	0.6	0.1 [a]	0.1	6.4	40.3			(Tartakovsky et al., 2009)
			0.55	1.4	1.12 [a]	1	1.8	51.2			
			0.7	2.5	3.11 [a]	2.1	1.5	65			
			0.74	3.2	3.65 [a]	2.2	1.7	61.1			
			0.85	3.2	3.66 [a]	2.6	1.9	71.9			
			1	4.7	6.9 [a]	3.9	1.8	90.6			
			1.15	4.2	6.22 [a]	3.8	2	89.6			
			0.4	0.4	0 [a]	-	-	61.9			
			0.55	1.2	0.33 [a]	0.6	5.3	68.5			
			0.7	1.4	0.59 [a]	0.7	4.4	59.1			
			0.85	1.6	0.85 [a]	1.3	4.2	68.3			
			1	1.8	1.33 [a]	1.4	3.5	60			
			1.15	1.8	1.14 [a]	1.3	4.8	62.4			
Carbon felt	GDC	Sodium acetate: 90.7 g/L ,Acetate load of 4.0 g/L/d (pump rate: acetate solution: 5.0 mL/d, trace metals dilution solution: 200 mL/d)	1	3.6	0	1.3	12.2				(Hrapovic et al., 2010)
	GDC/0.5 Pt			3.8	2.94	1.8	3.1				
	GDC/0.22 Ni,0.24 Pt			3.8	4.12	2.9	2.2				
	GDC/0.058 Ni			4.6	5.22	3.36	2.1				
	GDC/0.22 Ni			4	4.08	2.99	2				
	GDC/0.38 Ni			4.5	4.45	2.75	2.4				
	GDC/0.98 Ni			4.3	3.49	2.5	3				

Table 2.3 – (Continued) Design and performance of MEC with gas-phase cathode in continuous-flow mode

System Description			System Performances								
Anode	Carbon Cloth Based Gas Diffusion Cathode(GDC)/metal mg/cm2	Carbon Source	Eap (V)	I_A (A/m2)	Q_{H2} (L/ L/d)	Y_{H2} (mol/mol)	Win (Wh/ L)	η_{COD} (%)	CE (%)	η_E (%)	Ref
Carbon felt	GDC/0.22 Ni, 0.24 Pt	Sodium acetate: 90.7 g/L, Acetate load 5.8 g/L/d (pump rate: 7.5 mL/d; trace metals dilution solution: 200 mL/d)	1	4.8	4.2	2.85	2.7				(Hrapovic et al., 2010)
	GDC/0.058 Ni			4.4	5.02	2.5	2.1				
	GDC/ 0.22 Ni			4.6	5.4	3.3	2				
	GDC/0.38 Ni			5.7	5.16	3.14	2.6				
	GDC/0.98 Ni			5.4	4.68	2.57	2.8				
Graphite felt	carbon cloth GDC	Sodium acetate: 90.7 g/L, Acetate load 4.0 g/L/d (pump rate: 5.0 mL/d; trace metals dilution solution: 180-190 mL/d, HRT=6.3-6.7 h; Recirculation: 0.57 L/h)	1	2.47	0.02	0			56.6		(Manuel et al., 2010)
	GDC/0.3 Pt			2.9	2.61	2.4			75.3		
	GDC/0.65 Ni, 0.1 Mo, 0.2 Cr, 0.03 Fe			3.54	3.72	2.6			69		
	GDC/0.75 Ni, 0.228Cr, 0.027 Fe			4.09	3.25	2.4			77.3		
	GDC/0.61Ni, 0.34 Cr, 0.01Mn			3.39	2.77	1.9			64.9		
	GDC/0.4 Ni			2.69	2.85	1.9			51		
	GDC/ 0.6 Ni			3.6	4.14	2.8			68		
Graphite felt	GDC/ 0.4 Ni	DWW [1], OLR = 0.243 g COD/L/d, HRT=48 h	1	0.75 [b]				67	65		(Escapa et al., 2012)
		DWW [1], OLR = 0.448 g COD/L/d, HRT=24 h		0.79 [b]	0.12 [c]			62	59		
		DWW [1], OLR = 0.62 g COD/L/d, HRT=12 h		0.67 [b]	0.15 [c]			58	57		
		DWW [1], OLR = 1.24 g COD/L/d, HRT=6 h		0.34 [b]	0.22 [c]			61	55		
		DWW [1], OLR = 1.944 g COD/L/d, HRT=6 h		0.27 [b]	0.27 [c]			51	54		
		DWW [1], OLR = 3.128 g COD/L/d, HRT=3 h		0.19 [b]	0.32 [c]			44	38		

Table 2.3 – (Continued) Design and performance of MEC with gas-phase cathode in continuous-flow mode

System Description			System Performances								
Anode	Carbon Cloth Based Gas Diffusion Cathode(GDC)/metal mg/cm2	Carbon Source	Eap (V)	I_A (A/m2)	Q_{H2} (L/ L/d)	Y_{H2} (mol/mol)	E_I (Wh/ L)	η_{COD} (%)	CE (%)	η_E (%)	Ref.
Graphite felt	GDC/ 0.4 Ni	SWW [2], OLR = 6.4 g COD/L/d, HRT = 8 h	0.6		0.15 [b]			131.3	7.8		(Escapa et al., 2013)
			0.8		0.58 [b]				18.7	107.6	
			1		0.98 [b]				23.3	94.3	
		SWW [2], OLR = 6.4 g COD/L/d, HRT=10 h	0.6		0.20 [b]				10.9	129.9	
			0.8		0.64 [b]				14.5	106.8	
			1		1.28 [b]				23.2	96.2	
		SWW [2], OLR = 6.4 g COD/L/d, HRT=12 h	0.6		0.23 [b]				6.9	127	
			0.8		0.76 [b]				16.1	106.4	
			1		1.42 [b]				24.5	97	

a. calculated based on idea gas low, converted from data got at 273 K to 273.15 K

b. data read from the figure in the paper

c. calculated based on the Monod equation provided in the paper

DWW [1]. domestic wastewater range from 391 to 486 mg/L COD

SWW [2]. synthetic dark fermentation effluent: Acetate: 0.8-1.2 g/L, Propionate: 0.6-0.8 g/L, Butyrate: 0.2-0.4 g/L. a constant OLR of 6.4 g COD/L/d for all HRT tested

2.4.3 Up-flow continuous-flow system

Wang et al. (2012) developed a new membrane-free bioelectrochemical system, a membrane-free named, biocatalyzed electrolysis reactor (UBER), where the influent flows upwards through the cathode chamber that served primarily to mitigate inhibition of ARB, as depicted in Figure 2.6. The aforementioned authors used carbon brush as the anode, which was fixed on the upper portion of the reactor, and graphite granules as the cathode, which was 2 cm below the anode chamber. To ensure even distribution of up-flow fluid, two plates with even distribution holes were installed at the top and bottom of the reactor. They used this reactor to reduce nitrobenzene (Rodriguez et al., 2002) with acetate as the sole electron donor and carbon source. Nitrobenzene (NB) was efficiently removed (>99%) with aniline as the major product (>80%) in the cathode. The aniline can be degraded in natural ecosystems or wastewater treatment system under aerobic or denitrifying condition (Alexandra De et al., 1994). The nitrobenzene removal rate was 3.5 mol m^{-3} d^{-1}. The molar ratio of NB removed to acetate consumed varied from 4.3 ± 0.4 to 2.3 ± 0.1 mol mol^{-1}, 3-6 times higher than the theoretical value. Additional energy requirement was less than 0.075 KWh mol^{-1} NB.

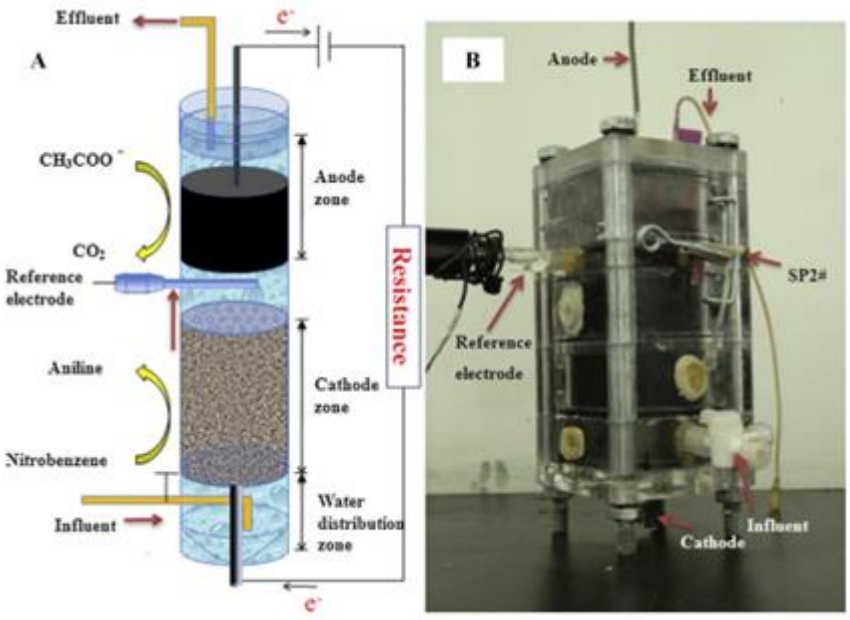

Figure 2.6 – Design of up-flow biocatalyzed electrolysis reactor (UBER). Left: Schematic diagram of the system. Right: Laboratory scale reactor for NB reduction (Wang et al., 2012)

Cui et al. (2012) also used the UBER to evaluate the reduction efficiency of azo dyes and assess the effects of hydraulic retention time on decolourization efficiency of azo dyes. Azo dyes were efficiently removed (94.8 ± 1.5%) at an HRT of 2 h and a loading rate of 780 g of alizarin yellow r (AYR) m^{-3} d^{-1}. The two main reductive products of azo dyes, phenylenediamine and 5-aminosalicylic acid, were subsequently oxidized in their lab scale aerobic biological oxidation reactor to simple acids and alcohols.

These results indicate the feasibility of the UBER as a single reactor with anodic biological and cathodic electrochemical functions. The biggest advantage of this design is the mitigation of toxicity to the electrogenic microorganism on the anode, since before going through the anode, the inhibitory chemicals were already reduced to less- or non-

toxic forms in the lower cathode chamber. The greatest challenge of this reactor was bacterial migration from the anode to the cathode caused by the lack of membrane. Even though the migration rate is slow, further research needs to be conducted to examine whether the biocathode could enhance the performance of this system.

2.4.4 Biocathode

Luo et al. (2014) studied a two-chamber MEC with sulfate reducing bacteria (SRB) biocathode to explore the potential of treating sulfate-rich wastewater and evaluated batch and continuous-flow performance. The schematic design of the aforementioned system is shown in Figure 2.6. To acclimate the SRB, domestic wastewater was used as inoculum and fed with sulfate medium in anaerobic batch reactors. The autotrophic SRB was considered to be dominant in the wastewater when sulfate removal rate was stable. The cathode chamber was filled with 1 g L^{-1} of sodium acetate medium while the catholyte consisted of 100 mg L^{-1} sulfate medium. In the continuous-flow mode, the current density reached 50 A m^{-3}, and the sulfate reduction rate reached 5.81 ± 0.38 mg d^{-1} nearly 11 times that of the fed-batch operation.

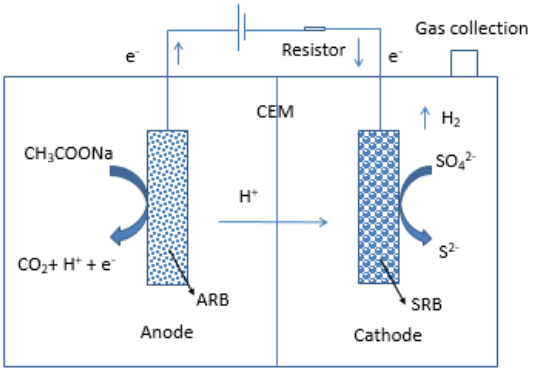

Figure 2.7 – Schematic diagram of the SRB-biocathode MEC. (Modified from Luo et al., 2014)

Thrash et al (2007) also studied biocathodes by introducing dissimilatory perchlorate reducing bacteria (DPRB) to the anode. They investigated the reduction of perchlorate, which is a very stable contaminant, in the cathodic chamber of a bioelectrical reactor. Both pure culture of DPRB and natural DPRB populations were tested in this experiment. The results showed that *Dechloromonas* and *Azospira* species in the pure culture of DPRB readily reduced 90 mg L^{-1} perchlorate in this system with 2,6-anthraquinone disulfonate (AQDS) as a mediator. When a natural microbial community was inoculated into the fed-batch bioelectrical reactor, a novel DPRB, strain VDY, was isolated which readily reduced perchlorate in a mediator-less reactor. In the continuous-flow up-flow mode, perchlorate removal efficiency reached 95% at a perchlorate loading rate of 60 mg L^{-1} day^{-1}. These results demonstrated the potential for application of bioelectrical reduction for the treatment of perchlorate contamination.

2.5 Combined processes

The anaerobic baffled reactor (ABR) a series of up-flow anaerobic sludge bed (UASB) reactors may potentially play an important role in wastewater treatment. Ran et al. (2014) developed a new process to enhance the stability and efficiency of ABR by combining it with MECs, as shown in Figure 2.8. The lab scale ABR (3.46 L) was divided into four equal compartments by vertical baffles. The anode and cathode were fixed in the last three compartments with an applied voltage of 0.9 V and an HRT of 24 h. The influent COD ranged from 1200 mg L^{-1} to 3500 mg L^{-1} with glucose as substrate. This combined reactor generated both methane and hydrogen, with the hydrogen fraction of biogas in the first compartment of 20.7% and methane content of 98.8%, 93.6% and 70.1% in the last three compartments, and achieved 98% COD removal efficiency.

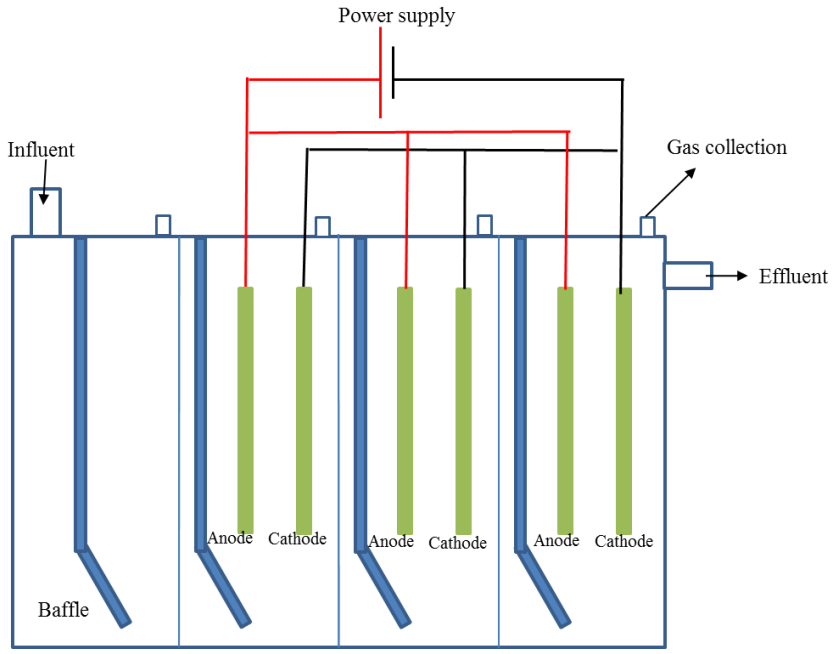

Figure 2.8 – The structure of anaerobic baffled reactor combining with microbial electrolysis cells. (Modified from Ran et al., 2014)

2.6 Pilot-scale continuous-flow microbial electrolysis cell

A pilot-scale (1,000 L) continuous-flow microbial electrolysis cell was constructed and tested for current generation and COD removal with winery wastewater (Cusick et al., 2011). The reactor contained 144 electrode pairs in 24 modules with applied voltage of 0.9 V. The anode were made of heat treated graphite fiber brushes, and the cathode were stainless steel mesh. SCOD removal efficiency reached 62% at an HRT of 1 day. The maximum current density reached 7.4 A m^{-3} after 100 days, with a maximum gas production rate of 0.19 ± 0.04 L L^{-1} d^{-1}, containing 86% of methane.

Heidrich et al. (2014) operated a 100 L MEC for 12 month fed with raw domestic wastewater at ambient temperatures ranging from 1 °C to 22 °C, producing an average of 0.6 L d^{-1} of hydrogen. The MEC reactor contained 6 individual electrolysis cell and were placed in series. The wastewater was fed into the MEC reactor at 0.07 mL min^{-1}

corresponding to a hydraulic retention time of 1 day with an influent COD ranging between 147 and 1976 mg L^{-1}. The aforementioned authors found that there was a reduction in the total volume of hydrogen produced throughout the period, from July to December, an average of 0.8 L d^{-1} of hydrogen was produced, while from December to June, an average of 0.4 L d^{-1} hydrogen production was achieved. COD removal efficiency was highly variable, sometimes reaching over 60%, sometimes lower than 30%. The aforementioned authors also found that to maintain the MEC working in ambient temperature, microbial cultures from the local wastewater treatment plant should be used as the seed since they were already adapted to the ambient temperatures.

The two main challenges of the scaled-up process are the slow start-up time, requiring as long as 60 days for the exoelectrogenic biofilm to develop and grow on the anode, and the low hydrogen production.

2.7 Summary

Microbial electrolysis cell (MEC) is a very promising technology, since it can convert organic waste to hydrogen with only a small energy input. There are several parameters that can affect the performance of the MEC, such as the materials being used (e.g., anode, cathode, and membrane); the MEC configuration; substrate composition; the applied voltage; the controlled anode potential; as well as the feeding mode (batch or continuous mode). Carbon, low price metals, and anion exchange membrane are widely used materials for anode, cathode and membrane, respectively. While traditionally MECs have been run in a fed-batch mode, the application of the MEC to operate in continuous-flow mode has become very popular, which includes combining MEC with other wastewater treatment processes, increasing number of anode electrodes to increase the anode surface area, and incorporation of a penetrating anode chamber on top of cathode

chamber, etc. The continuous-flow mode can help MEC achieve better performance than batch mode since the organic loading rate can be controlled to preclude substrate limitations.

Running the MECs in continuous-flow mode is a fundamental step for the scalability of MEC technology. The main challenge for MECs scaling up is to achieve higher hydrogen production rate with lower energy input. To overcome the challenge and commercialize the MEC technology will require the development of effective ARBs, efficient cathode electrode materials, minimization of the internal losses which refers to the modification of the MEC architecture, and also integration of different wastewater treatment processes with MECs.

2.7 Reference

1. Alexandra De, M., O'Connor, O.A., Kosson, D.S. 1994. Metabolism of aniline under different anaerobic electron-accepting and nutritional conditions. Environ. Toxicol. Chem., 13, 233-239.

2. Call, D., Logan, B.E. 2008. Hydrogen production in a single chamber microbial electrolysis cell lacking a membrane. Environ. Sci. Technol., 42, 3401-3406.

3. Cheng, S., Logan, B.E. 2007. Ammonia treatment of carbon cloth anodes to enhance power generation of microbial fuel cells. Electrochem. Commun., 9, 492-496.

4. Cui, D., Guo, Y.-Q., Cheng, H.-Y., Liang, B., Kong, F.-Y., Lee, H.-S., Wang, A.-J. 2012. Azo dye removal in a membrane-free up-flow biocatalyzed electrolysis reactor coupled with an aerobic bio-contact oxidation reactor. J. Hazard. Mater., 239, 257-264.

5. Cusick, R.D., Ullery, M.L., Dempsey, B.A., Logan, B.E. 2014. Electrochemical struvite precipitation from digestate with a fluidized bed cathode microbial electrolysis cell. Water Res., 54, 297-306.

6. Cusick, D.R., Bryan, B., Parker, D.S., Merrill, M.D., Mchanna, M., Diely, P.D., Liu, G., Logan, B.E., 2011. Performance of a pilot-scale continuous flow microbial electrolysis cell fed winery wastewater. Bioenergy and Biofuels., 89, 2053-2063.

7. Dennis, P.G., Guo, K., Imelfort, M., Jensen, P., Tyson, G.W., Rabaey, K. 2013. Spatial uniformity of microbial diversity in a continuous bioelectrochemical system. Bioresour. Technol., 129, 599-605.

8. Dhar, B.R., Gao, Y., Yeo, H., Lee, H.-S. 2013. Separation of competitive microorganisms using anaerobic membrane bioreactors as pretreatment to microbial electrochemical cells. Bioresour. Technol., 148, 208-214.

9. Escapa, A., Gil-Carrera, L., García, V., Morán, A. 2012. Performance of a continuous flow microbial electrolysis cell (MEC) fed with domestic wastewater. Bioresour. Technol., 117, 55-62.

10. Escapa, A., Lobato, A., García, D., Morán, A. 2013. Hydrogen production and COD elimination rate in a continuous flow microbial electrolysis cell: The influence of hydraulic retention time and applied voltage. Environmental Progress & Sustainable Energy, 32, 263-268.

11. Gorby, YA., Yamina, S., Mclean JS et al. 2006. Electrically conductive bacterial nanowires produced by *Shewanella oneidensis* strain MR-1 and other microorganisms. P. Natl. Acad. Sci. USA. 103, 11358-11363

12. Gusseme, B.D., Soetaert, M., Hennebel, T., Vanhaecke, L., Boon, N., Verstraete, W. 2012. Catalytic dechlorination of diclofenac by biogenic palladium in a microbial electrolysis cell. Microbial biotechnology, 5, 396-402.

13. Hernandez, ME., Kappler, A, Newman, DK., 2004. Phenazines and other redox-active antibiotics promote microbial mineral reduction. Appl. Environ. Microb. 20, 921-928.

14. Hrapovic, S., Manuel, M.-F., Luong, J., Guiot, S., Tartakovsky, B. 2010. Electrodeposition of nickel particles on a gas diffusion cathode for hydrogen production in a microbial electrolysis cell. Int. J. Hydrogen Energy, 35, 7313-7320.

15. Hu, H., Fan, Y., Liu, H. 2008. Hydrogen production using single-chamber membrane-free microbial electrolysis cells. Water Res. 42, 4172-4178.

16. Hu, H., Fan, Y., Liu, H. 2009. Hydrogen production in single-chamber tubular microbial electrolysis cells using non-precious-metal catalysts. Int. J. Hydrogen Energy, 34, 8535-8542.

17. Jeremiasse, A.W., Hamelers, H.V., Saakes, M., Buisman, C.J. 2010. Ni foam cathode enables high volumetric H 2 production in a microbial electrolysis cell. Int. J. Hydrogen Energy, 35, 12716-12723.

18. Kadier, A., Simayi, Y., Kalil, M.S., Abdeshahian, P., Hamid, A.A. 2014. A review of the substrates used in microbial electrolysis cells (MECs) for producing sustainable and clean hydrogen gas. Renewable Energy, 71, 466-472.

19. Kundu, A., Sahu, J.N., Redzwan, G., Hashim, M. 2013. An overview of cathode material and catalysts suitable for generating hydrogen in microbial electrolysis cell. Int. J. Hydrogen Energy, 38, 1745-1757.

21. Lee, H.-S., Rittmann, B.E. 2009. Significance of biological hydrogen oxidation in a continuous single-chamber microbial electrolysis cell. Environ. Sci. Technol., 44, 948-954.

22. Lee, H.-S., Vermaas, W.F., Rittmann, B.E. 2010. Biological hydrogen production: prospects and challenges. Trends Biotechnol., 28, 262-271.

23. Liu, W., Wang, A., Ren, N., Zhao, X., Liu, L., Yu, Z., Lee, D., 2008. Electrochemically assisted biohydrogen production from acetate. Energy Fuels. 22, 159-163

24. Liu, H., Hu, H., Chignell, J., Fan, Y. 2010. Microbial electrolysis: novel technology for hydrogen production from biomass. Biofuels, 1, 129-142.

25. Logan, B.E., 2008a. Microbial Fuel Cells. John Wiley and Sons, Inc., Hoboken, New Jersey.

26. Logan, B.E., Call, D., Cheng, S., Hamelers, H.V., Sleutels, T.H., Jeremiasse, A.W., Rozendal, R.A. 2008b. Microbial electrolysis cells for high yield hydrogen gas production from organic matter. Environ. Sci. Technol., 42, 8630-8640.

27. Luo, H., Fu, S., Liu, G., Zhang, R., Bai, Y., Luo, X. 2014. Autotrophic biocathode for high efficient sulfate reduction in microbial electrolysis cells. Bioresour. Technol., 167, 462-468.

28. Manuel, M.-F., Neburchilov, V., Wang, H., Guiot, S., Tartakovsky, B. 2010. Hydrogen production in a microbial electrolysis cell with nickel-based gas diffusion cathodes. J. Power Sources, 195, 5514-5519.

29. Nam, J.-Y., Tokash, J.C., Logan, B.E. 2011. Comparison of microbial electrolysis cells operated with added voltage or by setting the anode potential. Int. J. Hydrogen Energy, 36, 10550-10556.

30. Nam, J.Y., Yates, M.D., Zaybak, Z., Logan, B.E. 2014. Examination of protein degradation in continuous flow, microbial electrolysis cells treating fermentation wastewater. Bioresour. Technol., 171, 182-186.

30. Newman DK, Kolter R., 2000. A role for excreted quinones in extracecullar electron transfer. Nature. 405, 94-94.

31. Rabaey, K., Van de Sompel, K., Maignien, L., Boon, N., Aelterman, P., Clauwaert, P., De Schamphelaire, L., Pham, H.T., Vermeulen, J., Verhaege, M. 2006. Microbial fuel cells for sulfide removal. Environ. Sci. Technol. 40, 5218-5224.

32. Rader, G.K., Logan, B.E. 2010. Multi-electrode continuous flow microbial electrolysis cell for biogas production from acetate. Int. J. Hydrogen Energy, 35, 8848-8854.

33. Ran, Z., Gefu, Z., Kumar, J.A., Chaoxiang, L., Xu, H., Lin, L. 2014. Hydrogen and methane production in a bio-electrochemical system assisted anaerobic baffled reactor. Int. J. Hydrogen Energy, 39, 13498-13504.

34. Refuera G., McCarthy KD., Mehta T., Nicoll JS., Tuominen MT., Lovely DR., 2005. Extracellular electron transfer via microbial nanowires. Nature. 435, 1098-1101.

35. Rodriguez, M., Timokhin, V., Michl, F., Contreras, S., Gimenez, J., Esplugas, S. 2002. The influence of different irradiation sources on the treatment of nitrobenzene. Catal. Today, 76, 291-300.

36. Rozendal, R.A., Hamelers, H.V.M., Buisman, C.J.N., 2006. Effects of membrane cation transport on pH and microbial fuel cell performance. Environ. Sci. Technol. 40, 5206–5211

37. Rozendal, R.A., Hamelers, H.V., Molenkamp, R.J., Buisman, C.J. 2007. Performance of single chamber biocatalyzed electrolysis with different types of ion exchange membranes. Water Res., 41, 1984-1994.

38. Selembo, P.A., Merrill, M.D., Logan, B.E. 2009. The use of stainless steel and nickel alloys as low-cost cathodes in microbial electrolysis cells. J. Power Sources, 190, 271-278.

39. Sleutels, T.H., Lodder, R., Hamelers, H.V., Buisman, C.J. 2009. Improved performance of porous bio-anodes in microbial electrolysis cells by enhancing mass and charge transport. Int. J. Hydrogen Energy, 34, 9655-9661.

40. Sleutels, T.H., Ter Heijne, A., Buisman, C.J., Hamelers, H.V. 2013. Steady-state performance and chemical efficiency of Microbial Electrolysis Cells. Int. J. Hydrogen Energy, 38, 7201-7208.

41. Tartakovsky, B., Manuel, M.-F., Wang, H., Guiot, S. 2009. High rate membrane-less microbial electrolysis cell for continuous hydrogen production. Int. J. Hydrogen Energy, 34, 672-677.

42. Thrash, J.C., Van Trump, J.I., Weber, K.A., Miller, E., Achenbach, L.A., Coates, J.D. 2007. Electrochemical stimulation of microbial perchlorate reduction. Environ. Sci. Technol, 41, 1740-1746.

43. Turick EK., Tisa LS., Caccavo F., 2002. Melanin production and use as a soluble electron shuttle for Fe oxide reduction and as a terminal electron acceptor by *Shewanella algae* BRy. APPL. Environ. Microb. 68, 2436-2444.

44. Villano, M., Aulenta, F., Beccari, M., Majone, M. 2012. Start-up and performance of an activated sludge bioanode in microbial electrolysis cells. Chem. Eng. (Mew York), 27.

45. von Canstein H., Ogawa J., Shimizu S, Lloyd Jr., 2008. Secretion of flavins by *Shewanella* species and their role in extracellular electron transfer. APP. Environ. Microb.,74, 615-623.

46. Wang, A.-J., Cui, D., Cheng, H.-Y., Guo, Y.-Q., Kong, F.-Y., Ren, N.-Q., Wu, W.-M. 2012. A membrane-free, continuously feeding, single chamber up-flow biocatalyzed electrolysis reactor for nitrobenzene reduction. J. Hazard. Mater., 199, 401-409.

47. Wang, A., Liu, W., Ren, N., Cheng, H., Lee, D.-J. 2010. Reduced internal resistance of microbial electrolysis cell (MEC) as factors of configuration and stuffing with granular activated carbon. Int. J. Hydrogen Energy, 35, 13488-13492.

48. Wang, X., Cheng, S., Feng, Y., Merrill, M.D., Saito, T., Logan, B.E. 2009. Use of carbon mesh anodes and the effect of different pretreatment methods on power production in microbial fuel cells. Environ. Sci. Technol, 43, 6870-6874.

49. Zhao, F., Harnisch, F., Schro¨der, U., Scholz, F., Bogdanoff, P., Herrmann, I., 2006. Challenges and constraints of using oxygen cathodes in microbial fuel cells. Environ. Sci. Technol. 40, 5193–5199.

Chapter 3

Impact of Volatile Fatty Acids on Microbial Electrolysis Cell Performance

3.1 Introduction

Hydrogen plays a key role in sustainable energy production. Although hydrogen can be recovered by fermentation of organic material rich in carbohydrates, the majority of organic matter remains in the form of volatile fatty acids (VFAs). The primary fermentation end products during biohydrogen production are acetic, butyric, and propionic acids (Liu et al., 2005a). To achieve a higher conversion of a substrate to hydrogen, an additional to fermentation to achieve a higher hydrogen yield is the process of electrohydrogenesis using microbial electrolysis cells (MECs). Anode-respiring bacteria (ARB), such as *Geobacter Shewanella, Clostridium, Pseudomonas, Desulfuromonas, Eseherichia,* and *Klebisella,* are able to transmit their electrons to a solid electron acceptor as part of their energy-generating respiration (Lee et al., 2010; Torres et al., 2007; Torres et al., 2010). Three mechanisms of extracellular electron transfer have been proposed, i.e., direct electron transfer, electron shuttle, and via a solid conductive matrix (Torres et al., 2010). The energy in the electrons can be utilized for electricity generation in a microbial fuel cell (MFC) (Logan et al., 2006) or for hydrogen gas production in a microbial electrolysis cell (MEC) (Liu et al., 2005b). In MECs, ARB are of special interest for oxidizing biodegradable organic compounds present in wastes and other forms of biomass into protons, electrons, and bicarbonate (Lee et al., 2010; Torres et al., 2007). The electrons reach the cathode and react with water to produce hydrogen. Hydrogen production using MECs has been studied using simple organic compounds, such as acetate, propionate, glucose, glycerol (Cheng and Logan, 2007; Lu et al., 2012;

Selembo et al., 2009; Sun et al., 2010); complex organic matter, such as starch, protein (Montpart et al., 2015; Nam et al., 2014); and real wastewater, for example, domestic wastewater, winery wastewater, and industrial wastewater (Cusick et al., 2011; Ditzig et al., 2007; Tenca et al., 2013).

Recently, combining dark fermentation with MECs seems to be very promising. Anode respiration process and fermentation can be combined in two different ways. One is adding the fermentative microorganisms and anode respiring bacteria in the same reactor to create a mixture of these two cultures in the MEC anode chamber. Montpart et al. (2015) obtained a group of microorganisms able to degrade a specific complex substrate (glycerol, milk and starch) by separately growing fermentative and ARB microbial communities in culture flasks and in an MFC respectively before combining both communities in a single chamber MEC. In this approach, they demonstrated that the growth of an anodic syntrophic consortium between fermentative bacteria and ARB was operationally enhanced and increased the potential of these complex substrates to be treated (Montpart et al., 2015). On the other hand, fermentation and hydrolysis could be separated into an independent reactor, with the MFC/MEC receiving simpler organic compounds typical of fermentation effluent, which are further consumed by ARB (Torres et al., 2007). For example, a two-stage dark-fermentation and electrohydrogenesis process was used to produce hydrogen gas by converting organic compounds such as cellulose (Lalaurette et al., 2009) and crude glycerol (Chookaew et al., 2014) to smaller compounds.

As the main end products from dark fermentation, VFAs have a vital impact on the performance of MECs. Escapa et al. (2013) found that acetate and butyrate were easily

degradable, whereas propionate exhibited pseudo-recalcitrant behavior in a continuous-flow two-chamber MEC fed with synthetic dark fermentation wastewater. However, this was contradictory to the findings of other groups. Li et al. (2014) indicated that the propionate had a higher priority sequence for hydrogen production than butyrate in a single-chamber MEC fed with corn stalk fermentation effluent. In their work, the removal efficiency of acetate, propionate and butyrate were reported as of 81-91 %, 11-16 % and 4%, respectively (Li et al., 2014). Torres et al. (2007) also demonstrated that acetate and propionate were consumed more effectively than the butyrate in the continuous-flow H-type MEC fed with a mixture of fermentation products. They reported a maximum current density for acetate of 9.0 A/m^2, 1.6 A/m^2 for propionate, and only 0.16 A/m^2 for butyrate. The detailed comparisons among the above studies are listed in Table 3.1. In order to clear this contradiction and figure out the impact of different VFAs on the MEC performance, this study compared MEC operational parameters by feeding the MEC with different VFAs, namely acetate, butyrate and propionate.

Table 3. 1 -- Summary of current densities and removal efficiencies by different authors using acetate, butyrate and propionate

Substrate	Running mode	MEC type	Applied voltage (V)(unless otherwise stated)	T[a] (°C)	pH	Influent component	Influent COD (mg/L)	Removal efficiency (%)	CD[d] (A/m^3)	HPR[c] ($m^3/m^3/d$)	Source
CSFE *	batch	single chamber	0.8	36	7	acetate butyrate propionate	1490[e] 1967[e] 45[e]	91 4 14[d]	340	3.43	Li et al. (2014)
SDFE §	continuous-flow	two chamber (gas cathode)	1	25	7	acetate butyrate propionate	1302[e] 736[e] 1227[e]	100 100 <100	206	1.42	Escapa et al. (2013)
SDFE §	continuous-flow	H-type dual-compartment	anode potential (+0.1 V vs Ag/AgCl)	30	7.4	acetate butyrate propionate	2560[e] 6400[e] 4480[e]		281[e] 5[e] 50[e]		Torres et al. (2007)

Note: T[a]: temperature; CD[b] current density; HPR[c]: hydrogen production rate; [d]: the data was gotten from the figure in the reference; [e]: the data was calculated based on the information in the literature; CSFE *: corn stalk fermentation effluent; SDFE §: synthetic dark fermentation effluent

3.2 Materials and methods

3.2.1 Reactor set-up

The MEC was fabricated from plexiglass with anode and cathode volumes of 550 mL and 225 mL, respectively. The liquid volume in the anode varied from 500 mL to 530 mL since some of the liquid was washed out with the purge of nitrogen. One bundle of high density carbon fibers (2293-B, 24K Carbon Tow, Fibre Glast Developments Corp., OH, USA) that was intertwined through holes drilled on a stainless steel frame was used as the anode module. The specific surface area of the fibers was 571429 m^2/m^3 (fiber's diameter, 7 µm; length, 150 cm). The bundle contained 24,000 individual carbon filaments with a geometric surface area of 7913 cm^2. The geometric surface area of the anodes per MEC anode volume was 1583 m^2/m^3. The carbon fibers were pretreated with nitric acid (1N), acetone (1N) and ethanol (1N) for 1 day each, and then washed with MilliQ water (18.2 MΩ-cm) (Dhar et al., 2013). The cathode electrode was made of a stainless steel mesh (Type 304, McMaster Carr, OH, USA). An anion exchange membrane (AMI-7001, Membrane International Inc., NJ, USA) was placed between the anode and the cathode as a separator, and the geometric surface area of the membrane was 18 cm^2. The membrane was pretreated at 40°C in 5% NaCl solution for 24 hours as per the manufacturer recommendations. To avoid possible short-circuiting and liquid leakage, non-conductive polyethylene mats were used between the electrodes and membrane (Dhar et al., 2013). The distance between the anode and cathode electrodes was less than 1 cm. A schematic and picture of the sandwich type anode-membrane-cathode are shown in Figure 3.1.

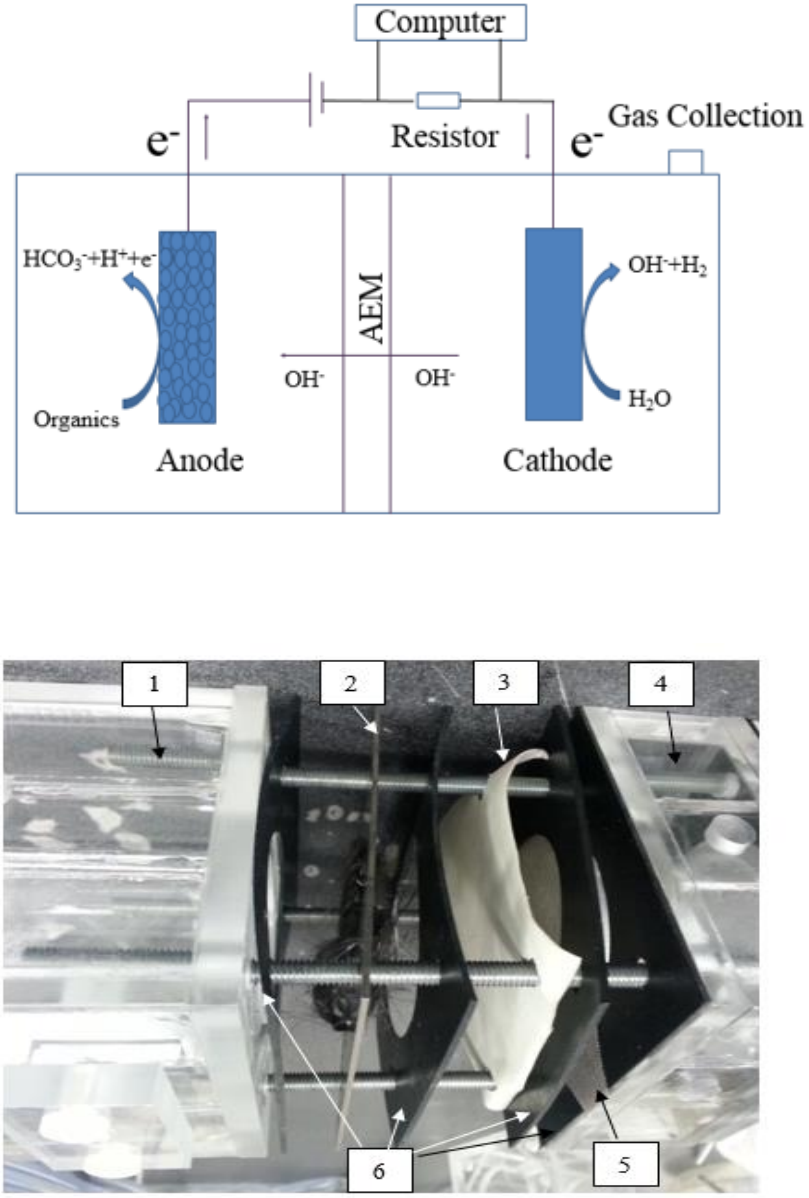

Figure 3.1 -- **a** – Schematic illustration of a typical two-chamber MEC with an anion exchange membrane (AEM); **b** – Picture of connecting the anode chamber (1), anode electrode (2), membrane (3), cathode chamber (4), cathode electrode (5), and non-conductive polyethylene (6) together

A voltage of 1.0 V was applied across the electrodes using a power supply (B&K Precision Corp., California, USA). The positive lead of the power supply was connected to the anode, and the negative lead was serially connected to a 10 Ω resistor and the cathode. The temperature was maintained at room temperature (25°C) during the whole experiment.

3.2.2 MEC inoculation and operation

The MEC was inoculated with 50 mL of effluent from a working MEC, which selectively enriched from activated sludge microbial consortium from Adelaide Wastewater Treatment Plant (London, CA) over a period of three months, during which the cultures were fed with acetate in batches. The anode chamber was fed with a medium containing 2.3 g/L KH_2PO_4, 4.66 g/L Na_2HPO_4, 0.038 g/L NH_4Cl and 0.84 g/L $NaHCO_3$ and 1 mL/L of a trace element mixture with the following composition: 25 mg/L $MgCl_2 \cdot 6H_2O$; 6 mg/L $MnCl_2 \cdot 4H_2O$; 1.2 mg/L $CaCl_2 \cdot 2H_2O$; 0.5 mg/L $ZnCl_2$; 0.11 mg/L $NiCl_2$; 0.1 mg/L $CuSO_4 \cdot 5H_2O$; 0.1 mg/L $AlK(SO_4)_2 \cdot 12H_2O$; 1 mg/L $Co(NO_3)_2 \cdot 6H_2O$; 0.1 mg/L H_3BO_3; 5 mg/L EDTA; 0.1 mg/L $Na_2WO_4 \cdot 2H_2O$; 0.1 mg/L $NaHSeO_3$; 0.2 mg/L $Na_2MoO_4 \cdot 2H_2O$. 20 mM $FeCl_2 \cdot 4H_2O$ and 77 mM $Na_2S \cdot 9H_2O$ were also added to the medium (1 mL/L) (Dhar et al., 2013; Torres et al., 2007). The substrate concentrations (added as sodium acetate, sodium propionate, sodium butyrate) are noted below. Medium pH was constant at 7.2 ± 0.2. The cathode chamber was filled with distilled water.

The MEC was carried out in batch mode. At least three consecutive batch cycles were achieved before changing the substrate. When the current dropped below 2 mA for acetate and butyrate-fed cycles, and 1 mA for propionate-fed cycles, the liquids in the anode and cathode chamber were emptied and refilled with the medium as described

above. 2 g/L sodium acetate (CH_3COONa) corresponding to a COD of 1600 mg/L was added during the star-up period and three consecutive cycles. Subsequently, 0.55 g/L sodium butyrate (C_3H_7COONa) were fed into the MEC. Finally, 0.686 g/L of sodium propionate (C_2H_5COONa) was added and the MEC was run for another three cycles. To reduce the cycle time, the influent COD of butyrate and propionate were both reduced to 800 mg/L. Ultra-pure nitrogen was sparged into the anode chamber for 20 min at the beginning of each batch cycle to ensure anaerobic conditions.

3.2.3 Analytical methods

The total volume of biogas produced from the MECs was measured using the water displacement method. The biogas composition including hydrogen, methane, and nitrogen was determined by a gas chromatograph (Model 310, SRI Instruments, Torrance, CA) equipped with thermal conductivity detector (TCD) and a molecular sieve column (Mole sieve 5A, mesh 80/100, 6 ft × 1/8 in) (Gupta et al., 2014). Argon was used as a carrier gas at a flow rate of 30 mL/min and the temperature of the column and thermal conductivity detector (TCD) detector were 90°C and 105°C, respectively. In the MEC, the voltage drop across the external resistor was measured using a multimeter with a data acquisition system (2700, Keithly Instruments Inc., Cleveland, Ohio), with the current calculated using Ohm's Law ($I = V/R$), where V was the measured voltage drop across the resistor ($R = 10\ \Omega$) (Rader & Logan, 2010). Total and soluble chemical oxygen demand (TCOD/SCOD) were measured using HACH methods and test kits (HACH Odyssey DR/2500 spectrophotometer manual). TSS and VSS were analyzed using standard method (APHA, 1998). pH was measured using a pH probe (SympHony B10P, VWR, Visalia, CA).

3.2.4 Calculations

3.2.4.1 Hydrogen recovery

Coulombic efficiency (C_E) was calculated on the basis of the measured current compared to the substrate removed using the following equations, (1-3):

$$C_E = \frac{n_{CE}}{n_{th}} = \frac{8 \cdot I_{AVG,90} \cdot t}{F \Delta SCOD} \quad (1)$$

$$n_{th} = \frac{2 \Delta SCOD}{M_{O2}} \quad (2)$$

$$n_{CE} = \frac{I_{AVG,90} t}{2F} \quad (3)$$

Where n_{CE} (mol) is the moles of hydrogen that could be recovered based on measured current, n_{th} (mol) is the maximum theoretical hydrogen potential from the SCOD removal, F is the Faraday constant (F = 96485 C/mole$^-$), ΔSCOD (g) is the soluble COD removed, and 8 is the conversion factor of COD to moles of electrons, M_{O2} (g/mol) is the molecular weight of oxygen, while the 2 in equation (2) is the number of moles of hydrogen that can be produced with each mole of SCOD consumed. $I_{AVG, 90}$ is the average current calculated over the time (t) for accumulation of 90% of the charge. The use of $I_{AVG, 90}$ is more accurate when analyzing MEC performance in a batch cycle because it eliminates the small current densities at the end of the cycle and focuses on the most useful part of the current generation cycle (Ivanov et al., 2013).

The cathodic hydrogen recovery (r_{cat}) was calculated using equation (4):

$$r_{cat} = \frac{n_{H2}}{n_{CE}} \quad (4)$$

Where n_{H2} (mol) is the actual moles of hydrogen recovered at the cathode.

The overall hydrogen recovery is (Logan et al., 2008): $R_{H2} = C_E r_{cat}$ (5)

Theoretical hydrogen yield (Y_{H2}) is based on the theoretical maximum production of hydrogen.

$$Y_{H2} = \frac{n_{H_2}}{n_{th}} \quad (6)$$

Where n_{th} is the maximum theoretical hydrogen (mol) based on SCOD removal.

Volumetric hydrogen production rate (HPR) (m^3 $H_2/m^3/d$) was normalized to the cathode liquid volume (225 mL).

3.2.4.2 Energy recovery

The energy recovered (η_E) based on the energy input was calculated using the following equation:

$$\eta_E = \frac{-W_{H_2}}{W_{in}} = \frac{n_{H2}\Delta H_{H2}}{E_{ap}It - I^2Rt} \quad (7)$$

Where W_{H2} (J) is the amount of energy recovered in hydrogen, W_{in} (J) is the electrical energy input, ΔH_{H2} (-285.8 J/mol) is the energy content of hydrogen based on the heat of combustion (Logan et al., 2008), E_{ap} (V) is the applied voltage to the system by the power supply, I (A) is the current during the batch cycle, R is the external resistor (10 Ω), and t (s) is the time of each batch cycle.

The energy recovered (η_{E+S}) based on both the energy input and the energy in the substrate was calculated using the following equation:

$$\eta_{E+S} = \frac{-W_{H_2}}{W_{in} - W_s} \quad (8)$$

Where Ws is the energy in the substrate which can be calculated similar to the energy content of hydrogen, i.e., $\Delta H_{Acetate}$ = -874.3 KJ/mol (Logan et al., 2008), $\Delta H_{Propionate}$= -1528.3 KJ/mol (Chadwick, 1988), $\Delta H_{Butyrate}$ = -2183.5 KJ/mol (Dorofeeva et al., 2001).

The current density (CD) (A/m^2 or A/m^3) was the current produced in the batch cycle per unit membrane surface area, or unit liquid volume.

3.3 Results and discussion

3.3.1 Effects of substrate on current density and hydrogen production rate

The profile of the batch current density fed with different substrates is illustrated in Figure 3.2. During the start-up period, the current stayed at zero for 24 hours, and then started to increase. For all other cycles, the current would increase directly (without lag phase) after feeding. This indicated that the anode respiring bacteria were effectively attached to the anode. When the MEC was fed with butyrate for the first time (cycle 5), the current increased smoothly peaking on day 51, 9 days after the butyrate feed, thus demonstrating that the ARB were adapting to the new substrate. In the last butyrate cycle, the current peaked only 24 hours after the feed. For all three butyrate batches, the maximum current was almost the same at 4.5 mA. After feeding the MEC with propionate, the current also increased very slowly and after 8 days achieved a lower maximum current of 3.0 mA. In the last cycle of the propionate-fed MEC (cycle 10), the current did not peak until after 8 days, which was the same as the first propionate cycle (cycle 8). The comparatively slower rate for the current to peak in the propionate-fed MEC denoted that the ARB cannot utilize propionate directly. It is more likely that the propionate was first oxidized to acetate by acetogenic bacteria, and then consumed by ARB. The average time for accumulation of 90% of the charge were 8.9 days for acetate,

9.1 for butyrate and 12 days for propionate. The longer time for propionate to accumulate 90 % of the charge was mainly due to the slower rate for the current density to peak.

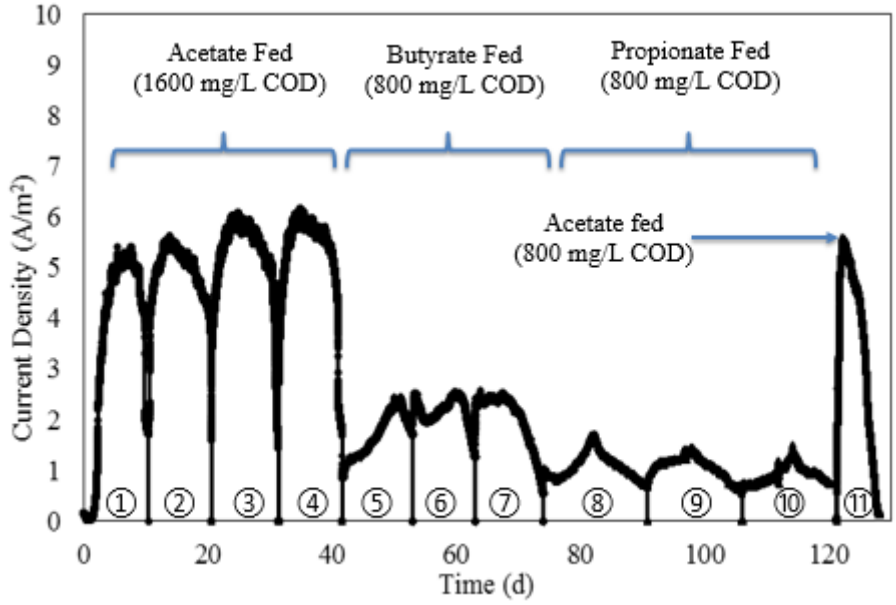

Figure 3.2 – The changes of current densities with different substrates, including: start-up cycle (1), acetate-fed cycles (2 to 4), butyrate-fed cycles (5 to 7), propionate-fed cycles (8 to 10), and acetate-fed cycle (11). The COD of cycle 1 to 4 are 1600 mg/L, and for cycle 5 to 11 are 800 mg/L.

The cycles fed with acetate had the highest peak of current density (6.0 ± 0.28 A/m^2), followed by the butyrate fed cycles (2.5 ± 0.06 A/m^2), and propionate fed cycles achieved the lowest current density (1.6 ± 0.14 A/m^2). The differences between the current densities might be attributed to a number of factors including the substrates order, the resistance of the membrane, pH gradient between the anode and cathode chambers, the influent COD (COD_{in}), and the substrate utilization rate. Of the aforementioned factors, the order of the feeding and the resistance of the membrane were discounted

because at the end of this experiment, the MEC was fed with acetate again at a concentration of 800 mg COD/L, and the current was almost the same as the current achieved at the beginning of this experiment (See Figure 3.2). The pH gradient was not a reason to cause these differences neither, since the pHs of the cathode were very close, i.e., 9.8 ± 1.7 for acetate, 9.7 ± 0.8 for butyrate, and 10.0 ± 0.4 for propionate. The anode pHs during the whole experimental period were maintained near neutral by the buffer in the medium. Even though the influent COD of acetate was different from that of butyrate and propionate, this could not cause the large difference in the maximum current densities between acetate and butyrate or propionate, because at the end of the experiment, when fed with 800 mg/L COD of acetate, the achieved current density was as high as 5.5 A/m^2, which was almost the same as MEC feeding with 1600 mg/L COD acetate. The reduced influent COD concentration only reduced the cycle time from 10.6 to 6.4 days. This is consistent with the findings of Liu et al. (2005a) who reported that the voltages generated in a microbial fuel cell (MFC) using acetate at different concentrations (from 80 mg/L to 800 mg/L) stayed at around 0.45 V. In addition, Oh et al. (2005) noted that the current density remained the same upon changing the influent propionate concentration from 0.26 mM to 0.53 mM. This clearly demonstrates that the only reason to limit the current densities in this case was the type of substrate. Acetate has been well known to be easily utilized by ARB, since it is not fermentable and has relatively rapid oxidation kinetics in MFC/MECs (Lee et al., 2009), while there has been no agreement on the relative biodegradability of butyrate and propionate. As the substrate-utilization rate is proportional to current density in an MEC (Lee and Rittmann., 2009), the utilization rate of the propionate (28 ± 0.8 mg COD/L/d) might have limited the current density, which was relatively low when compared with the average substrate utilization rate of acetate

(92 ± 5.0 mg COD/L/d) and butyrate (41 ± 4.8 mg COD/L/d). This indicated that the utilization rate of the substrates for ARB in MECs followed the order: acetate > butyrate > propionate.

As depicted in Figure 3.3, the type of substrate also has a significant impact on the hydrogen production rate. Similar to the trend of current density, the hydrogen production rate decreased from 0.50 ± 0.04 $m^3/m^3/d$ for acetate to 0.07 ± 0.01 $m^3/m^3/d$ for propionate. The current density and hydrogen production exhibited the same trend.

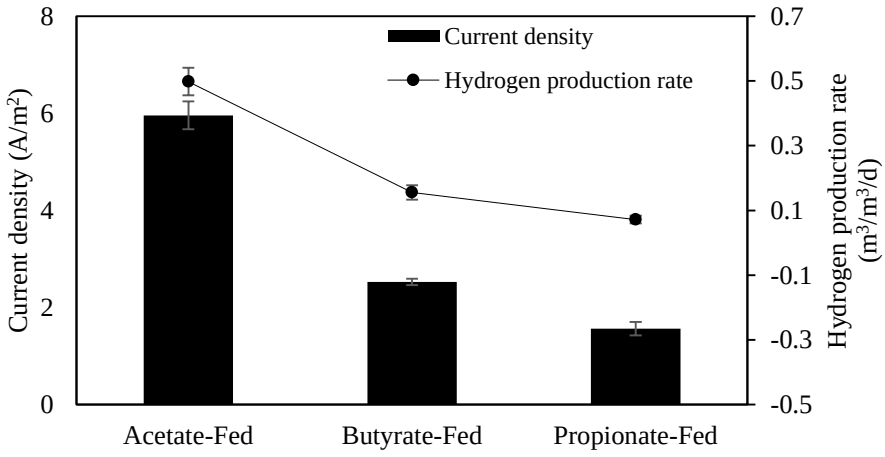

Figure 3.3 – The average current densities and hydrogen production rates in MEC fed with different substrates

3.3.2 Effects of substrate on hydrogen recovery and energy efficiency

Cathodic hydrogen recovery is a very important parameter to evaluate the MEC performance, since it takes into account the H_2 recovered at the cathode and the electrons transferred through the electrode. While indeed both electrodes appear independent, based on equation (4), the cathodic hydrogen recovery depends on both the hydrogen

recovery and the electron transferred from the anode to the cathode, which is influenced by the ARB activity, and hence varied from one substrate to another. According to the cathodic reaction, the more the electrons transferred to hydrogen, the higher the cathodic hydrogen recovery. In this study, the cathodic hydrogen recovery decreased in the order of feeding with acetate, butyrate and propionate as shown in Figure 3.4, which were 98 ± 0.8, 79 ± 4.9, and 71 ± 7.2 %, respectively. The differences in the cathodic hydrogen recoveries revealed that the electrons transferred to produce hydrogen for propionate was not as efficient as butyrate and acetate. The ratio of current density over hydrogen production rate exhibited an inverse linear relationship as shown in Figure 3.5.

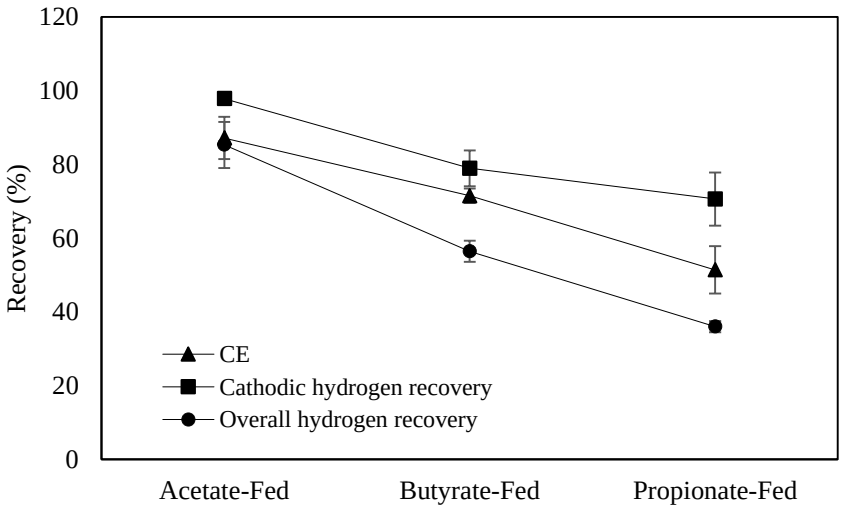

Figure 3.4 – The coulombic efficiencies (CE), cathodic hydrogen recoveries and overall hydrogen recoveries in MEC fed with different substrates

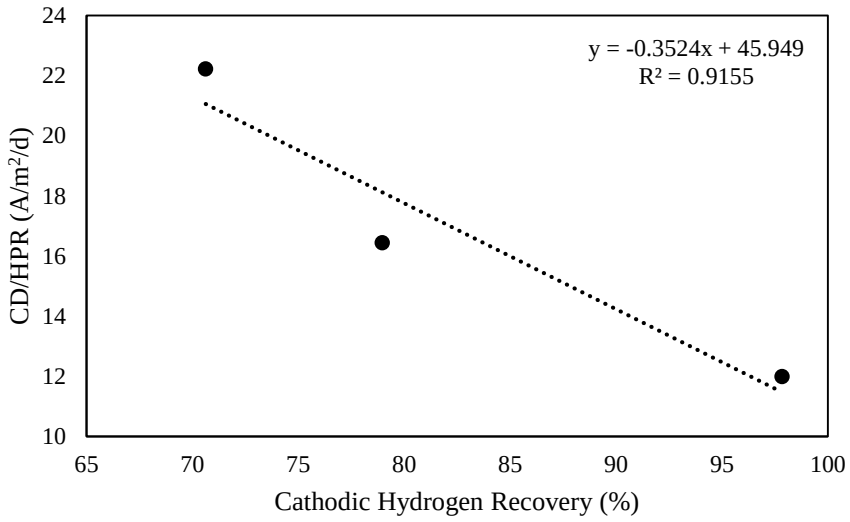

Figure 3.5 – The relationship of CD/HPR (current density/hydrogen production rate) and cathodic hydrogen recoveries in MEC fed with different substrates

The coulombic efficiencies for acetate, butyrate, and propionate were 87 ± 5.7, 72 ± 2.0 and 51 ± 6.4 %. These values are comparable with previous studies in continuous-flow mode MECs of 86 % for acetate (Torres et al., 2007), 41% for propionate (Torres et al., 2007); 23.6 ± 9.6 % from dark fermentation effluent reported by Chookaew et al. (2014). The overall H_2 recovery is the product of coulombic efficiency and cathodic hydrogen recovery from equation (5), so the overall H_2 recovery exhibited the same trend as both the coulombic efficiency and cathodic hydrogen recovery.

Table 3. 2 -- Comparison of key parameters reported in literatures versus data obtained in this study

Substrate	E_{ap} (V)	Y_{H2} (mol H_2/mol substrate)(unless otherwise stated)	R_{H2} (%)	HPR ($m^3/m^3/d$)	η_E (%)	η_{E+S} (%)	CD^a (A/m^3)	CD^b (A/m^2)	C_E (%)	Source
Acetic acid	0.8	3.65	91	1.1	260	82	99			Cheng and Logan (2007)
	0.5		53	0.02	169	53	2.8		92	Rozendal et al. (2006)
Sodium acetate	0.6		62	0.53	204	58	52		75	Hu et al. (2008)
	1		24	0.31			26		23	Rozendal et al. (2007)
	1	3.9		6.9*				4.7		Tartakovsky et al. (2009)
	1	1.4		1.33*				1.8		Tartakovsky et al. (2009)
	1	3.6	90	0.53	161	68	22.17	6.16	91	This study
Sodium butyrate	1	5.94	59	0.18	127	48	9.27	2.57	70	This study
Sodium propionate	1	2.56	37	0.072	112	43	5.26	1.46	59	This study
DFE [§]	1	27.93 mL H_2/g COD consumed	1.9	0.019			23.5		9.1	Chookaew et al. (2014)

Note: The data was the highest value chosen from each substrate-fed cycles. E_{ap}: applied voltage; Y_{H2}: the hydrogen yield based on substrate consumed; R_{H2}: overall hydrogen recovery; HPR :average hydrogen production rate; η_E: energy efficiency based on electric energy input; η_{E+S}: energy efficiency based on both energy input and the energy content in substrate; CD^a: current density based on anode liquid volume; CD^b: current density based on anode or membrane surface area; CE: coulombic efficiency; * : the data was calculated based on the information in the literature; [§]: dark fermentation effluent

The hydrogen yield and energy efficiency are shown in Figure 3.6. Theoretically, 4 moles of hydrogen are produced with 1 mole of acetate consumed according to equation (9). In this study, 3.4 ± 0.25 moles hydrogen per mole of acetate consumed were observed. This hydrogen yield corresponded to an energy recovery of 161 ± 1.4 % when evaluated in terms of only the voltage addition (1 V). For butyrate, the achieved hydrogen yield was 5.6 ± 0.29 mol H_2/mol butyrate, as compared with a theoretical value of 10 mol H_2/mol butyrate (Equation (10)). The energy efficiency for butyrate was 121 ± 7.3%. It should be noted that since the energy efficiency calculation was only based on the electrical input power, any values above 100% reflect energy recovery from the chemical substrate as well. These data are comparable with the reported performance in the literature (Table 3.2). In this study, a hydrogen yield of 2.46 ± 0.17 mol H_2/mol propionate was achieved as compared with a theoretical yield of 7 mol H_2/mol propionate (Equation (11)). The relatively lower observed hydrogen yield for propionate in this study is consistent with the literature. Moreover, the normalized hydrogen production per unit mass of soluble COD consumed (ΔSCOD) are 0.053 mol H_2/g ΔSCOD for acetate, 0.035 mol H_2/g ΔSCOD for butyrate and 0.022 mol H_2/g ΔSCOD for propionate, confirming that more soluble COD was oxidized to produce hydrogen from acetate and butyrate-fed cycles than from propionate-fed cycles.

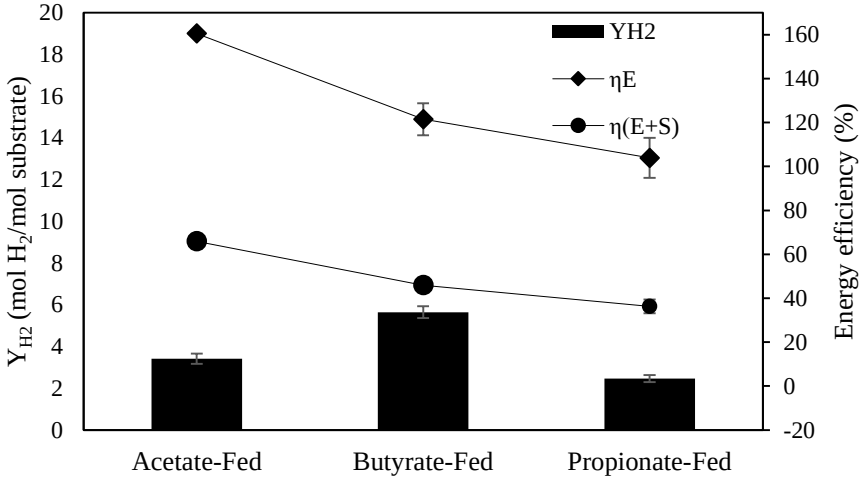

Figure 3.6 – The changes of hydrogen yields (Y_{H2}), energy efficiencies with only electric input (η_E), and energy efficiencies including both electric input and the energy content in substrate (η_{E+S}) in MEC fed with different substrates

Acetate as substrate:

$$1/8\ CH_3COO^- + 3/8\ H_2O \rightarrow 1/8\ CO_2 + 1/8\ HCO_3^- + H^+ + e^- \quad (9)$$

Butyrate as substrate:

$$1/20\ CH_3CH_2CH_2COO^- + 7/20\ H_2O \rightarrow 3/20\ CO_2 + 1/20\ HCO_3^- + H^+ + e^- \quad (10)$$

Propionate as substrate:

$$1/14\ CH_3CH_2COO^- + 5/14\ H_2O \rightarrow 1/7\ CO_2 + 1/14\ HCO_3^- + H^+ + e^- \quad (11)$$

3.3.3 Effects of substrate on COD removal and biomass production

Tables 3 and 4 describe the COD removal efficiencies together with a COD mass distribution for acetate, butyrate, and propionate. The start-up period was not included in this analysis. Almost all the SCOD was consumed (96 ± 1.7 %) in the acetate-fed MEC. This was consistent with the high hydrogen yield obtained in this study. The SCOD removal efficiencies for butyrate and propionate were 88 ± 5.3 and 87 ± 5.8 % respectively. The relatively lower SCOD removal efficiencies for butyrate and propionate compared with acetate was consistent with the measured current densities.

Table 3.3 -- COD data for each cycle

Substrate	TCOD initial (mg)	SCOD initial (mg)	TCOD final (mg)	SCOD final (mg)	SCOD Removed efficiency (%)	Average SCOD Removal efficiency (%)
Acetate-Fed	894.4	894.4	82.3	39.8	95.6	
	895.6	895.6	48.2	22.4	97.5	96 ± 1.7
	797.7	797.7	83.5	46.6	94.2	
Butyrate-Fed	420.1	420.1	102.6	74.2	82.3	
	408.1	408.1	58.8	39.8	90.3	88 ± 5.3
	424.9	424.9	89.0	32.9	92.3	
Propionate-Fed	401.9	401.9	70.7	26.8	93.3	
	419.0	419.0	129.2	72.6	82.7	87 ± 5.8
	397.8	397.8	109.1	63.6	84.0	

Table 3.4 -- COD mass distribution

COD sinks	Acetate-fed MEC		Butyrate-fed MEC		Propionate-fed MEC	
	COD (mg)	Fraction (%)	COD (mg)	Fraction (%)	COD (mg)	Fraction (%)
Initial COD	863	100	418	100	406	100
Final SCOD	36	4	49	12	55	14
H_2	655	76	208	50	124	31
Suspended biomass	35	4	34	8	49	12
Total COD out	726	84	292	70	227	56
Attached biomass	137	16	126	30	179	44

The possible COD sinks in this system were soluble microbial products (SMP), biomass (suspended and attached) and hydrogen. No methane was detected during the whole experiment. The initial TCOD was equal to the initial SCOD since the MEC were fed with synthetic solids-free substrates. The COD equivalent of hydrogen was calculated by equation (12), and the calculation for suspended biomass is in equation (13) (Lee et al., 2008). 1 mL of hydrogen is equivalent to 0.654 mg COD at room temperature (25°C). The suspended biomass was obtained from the COD data. The SMP was determined from the soluble COD. Thus, the only unknown COD sink is the attached biomass, which can be estimated from the COD mass balance. Without considering the COD from the attached biomass, the COD closure for acetate, butyrate and propionate-fed cycles were 84 ± 10.1, 70 ± 6.5 and 56 ± 4.7 %, respectively.

$$1\ \text{mL}\ H_2 = \frac{1\ \text{mmol}\ H_2}{22.4\text{mL}} \frac{273.15\text{K}}{298.15\text{K}} \frac{2\text{meq}\ e^-}{\text{mmol}\ H_2} \frac{8\ \text{mg COD}}{\text{meq}\ e^-} = 0.654\ \text{mg COD} \qquad (12)$$

$$\text{Suspended biomass} = (\text{TCOD} - \text{SCOD})_{\text{final}} - (\text{TCOD} - \text{SCOD})_{\text{initial}} \qquad (13)$$

The results showed that the suspended biomass in the acetate-fed MEC only accounted for 4% of the initial COD. Because the acetate is well known to be readily degradable by ARB, the acetate fed MEC is more favorable for ARB growth compared to acetogenic bacteria. In the acetate-fed MEC, the lower the suspended biomass the better, since it inferred that more ARB was attached. This was consistent with the higher current density achieved in acetate-fed MEC. The calculated suspended biomass yield and the estimated attached biomass in the acetate-fed MEC were 0.042 g biomass COD/g substrate COD and 0.166 g biomass COD/g substrate COD, respectively. These data are similar to the literature. Lee et al. (2008) observed a suspended biomass yield of 0.058 g

biomass COD/g acetate COD, and attached biomass yield of 0.117 g biomass COD/g acetate COD in a batch H-type MFC. However, with different substrate, the biomass growth would be highly different. For instance, the suspended and attached biomass observed for glucose by Lee et al. (2008), were 0.119 g biomass COD/g glucose COD, and 0.202 g biomass/g glucose COD, respectively, confirming that the substrate in MEC has a significant impact on the biomass yield and attachment. The biomass yields for butyrate-fed and propionate-fed MEC in this experiment are listed in Table 3.5.

Table 3.5 -- Average biomass yield based on the COD removed for each substrate

	Biomass Yield g biomass COD/g substrate COD		
	Acetate-fed	Butyrate-fed	Propionate-fed
Suspended biomass	0.042	0.092	0.140
Attached biomass	0.166	0.341	0.510
Total	0.208	0.433	0.650

The relatively higher biomass yields achieved in the propionate-fed and butyrate-fed MEC were contradictory with the relatively lower current densities than the acetate-fed MEC. These results emphasize that the butyrate and propionate could not be consumed by ARB directly. Instead, they were oxidized by acetogenic microorganisms first. In the propionate-fed and butyrate-fed MEC, the acetogenic microorganism became more active than in the acetate-fed MEC, and accordingly affected to the higher biomass yield. Even though the acetogenic microorganisms could oxidize propionate and butyrate, they could not transfer the electrons to the anode electrode, and therefore less current densities were observed. It is noteworthy that the ratio of suspended biomass to attached biomass was approximately 1:4 for all the three substrates, indicating that the attachment characteristics of the various microbial groups to the anode surface were similar since the

acetate-fed MEC biomass was predominantly ARB, while both the butyrate and propionate-fed MECs biomass comprised both acetogenic bacteria and ARB. Normalizing the maximum current density to the observed attached biomass is a measure of the activity of ARB and electron transfer capabilities, which as shown in Table 5, yields 43.8, 20.1 and 8.7 A/mg biomass COD/m^2 for the acetate-fed, butyrate-fed, and propionate-fed cycles. This reveals that potentially both the activity and electron transfer capabilities of the attached biomass in the butyrate-fed MEC was more than twice that of the propionate-fed MEC. These results further demonstrated that, compared with butyrate, propionate was more difficult to degrade in the MEC.

3.3.4 Comparison of the results in this study and the results in literatures

The performances of the MECs are largely depend on the MEC configuration, material, microorganism, pH, feeding conditions, and as well as substrate. It is very hard to make a comparison unless only one unknown is existed. In this research, all the other conditions are the same unless the substrate itself. As shown in Table 3.6, based on both the COD removal efficiencies and current densities, the butyrate feeding MEC can achieve a better performance than propionate feeding MEC.

Table 3.6 -- Summary of current densities and removal efficiencies by different authors using acetate, butyrate and propionate

Substrate	Running mode	MEC type	Applied voltage (V)(unless otherwise stated)	T[a] (°C)	pH	Influent component	Influent COD (mg/L)	Removal efficiency (%)	CD[d] (A/m^3)	Source
CSFE *	batch	single chamber	0.8	36	7	acetate	1490[e]	91	340	Li et al. (2014)
						butyrate	1967[e]	4		
						propionate	45[e]	14[d]		
SDFE §	continuous-flow	two chamber (gas cathode)	1	25	7	acetate	1302[e]	100	206	Escapa et al. (2013)
						butyrate	736[e]	100		
						propionate	1227[e]	<100		
SDFE §	continuous-flow	H-type dual-compartment	anode potential (+0.1 V vs Ag/AgCl)	30	7.4	acetate	2560[e]		281[e]	Torres et al. (2007)
						butyrate	6400[e]		5[e]	
						propionate	4480[e]		50[e]	
SDFE	batch	two chamber	1	25	7.2	acetate	1600	96	22.17	This study
						butyrate	800	88	9.27	
						propionate	800	87	5.26	

Note: T[a]: temperature; CD[b] current density; HPR[c]: hydrogen production rate; [d]: the data was gotten from the figure in the reference; [e]: the data was calculated based on the information in the literature; CSFE *: corn stalk fermentation effluent; SDFE §: synthetic dark fermentation effluent

3.4 Conclusion

This study mainly focused on the comparison of different parameters in MEC feed with different VFAs (acetate, butyrate and propionate). Each substrate was fed to the reactor for three consecutive-batch cycles. Of the three operational MECs, the acetate-fed MEC exhibited the best overall performance, whereas the propionate-fed MEC achieved the worst performance, which demonstrated that propionate could not be utilized by anode respiring bacteria as easily as butyrate. The ratio of the suspended biomass to attached biomass was approximately 1:4 for all the three substrates.

Acknowledgment

The authors would like to acknowledge NSERC CREATE for financial support. The authors also appreciate the kind and precious helps provided by Dr. Nakhla's research group and Western University.

3.5 References

1. American Public Health Association (APHA), 1998. Standard Methods for the Examination of Water and Wastewater,20th ed. Washington, DC, USA

2. Chadwick, S.S. 1988. Ullmann's Encyclopedia of Industrial Chemistry. Ref. Serv. Rev. 16, 31-34.

3. Cheng, S., Logan, B.E. 2007. Sustainable and efficient biohydrogen production via electrohydrogenesis. Proc. Natl. Acad. Sci. U.S.A. 104, 18871-18873.

4. Chookaew, T., Prasertsan, P., Ren, Z.J. 2014. Two-stage conversion of crude glycerol to energy using dark fermentation linked with microbial fuel cell or microbial electrolysis

cell. N. Biotechnol. 31, 179-184.

5. Cusick, R.D., Bryan, B., Parker, D.S., Merrill, M.D., Mehanna, M., Kiely, P.D., Liu, G., Logan, B.E. 2011. Performance of a pilot-scale continuous flow microbial electrolysis cell fed winery wastewater. Appl. Microbiol. Biotechnol. 89, 2053-2063.

6. Dhar, B.R., Gao, Y., Yeo, H., Lee, H.-S. 2013. Separation of competitive microorganisms using anaerobic membrane bioreactors as pretreatment to microbial electrochemical cells. Bioresour. Technol. 148, 208-214.

7. Ditzig, J., Liu, H., Logan, B.E. 2007. Production of hydrogen from domestic wastewater using a bioelectrochemically assisted microbial reactor (BEAMR). Int. J. Hydrogen Energy. 32, 2296-2304.

8. Dorofeeva, O., Novikov, V.P., Neumann, D.B. 2001. NIST-JANAF thermochemical tables. I. Ten organic molecules related to atmospheric chemistry. J. Phys. Chem. Ref. Data. 30, 475-513.

9. Escapa, A., Lobato, A., García, D., Morán, A. 2013. Hydrogen production and COD elimination rate in a continuous microbial electrolysis cell: The influence of hydraulic retention time and applied voltage. Environ. Prog. Sustain. Energy. 32, 263-268.

10. Gupta, M., Velayutham, P., Elbeshbishy, E., Hafez, H., Khafipour, E., Derakhshani, H., El Naggar, M.H., Levin, D.B., Nakhla, G. 2014. Co-fermentation of glucose, starch, and cellulose for mesophilic biohydrogen production. Int. J. Hydrogen Energy. 39, 20958-20967.

11. Hu, H., Fan, Y., Liu, H. 2008. Hydrogen production using single-chamber membrane-

free microbial electrolysis cells. Water Res. 42, 4172-4178.

12. Ivanov, I., Ren, L., Siegert, M., Logan, B.E. 2013. A quantitative method to evaluate microbial electrolysis cell effectiveness for energy recovery and wastewater treatment. Int. J. Hydrogen Energy. 38, 13135-13142.

13. Lalaurette, E., Thammannagowda, S., Mohagheghi, A., Maness, P.-C., Logan, B.E. 2009. Hydrogen production from cellulose in a two-stage process combining fermentation and electrohydrogenesis. Int. J. Hydrogen Energy. 34, 6201-6210.

14. Lee, H.-S., Parameswaran, P., Kato-Marcus, A., Torres, C.I., Rittmann, B.E. 2008. Evaluation of energy-conversion efficiencies in microbial fuel cells (MFCs) utilizing fermentable and non-fermentable substrates. Water Res. 42, 1501-1510.

15. Lee, H.-S., Rittmann, B.E. 2009. Significance of biological hydrogen oxidation in a continuous single-chamber microbial electrolysis cell. Environ. Sci. Technol. 44, 948-954.

16. Lee, H.-S., Torres, C.I., Rittmann, B.E. 2009. Effects of substrate diffusion and anode potential on kinetic parameters for anode-respiring bacteria. Environ. Sci. Technol. 43, 7571-7577.

17. Lee, H.-S., Vermaas, W.F., Rittmann, B.E. 2010. Biological hydrogen production: prospects and challenges. Trends Biotechnol. 28, 262-271.

18. Li, X.-H., Liang, D.-W., Bai, Y.-X., Fan, Y.-T., Hou, H.-W. 2014. Enhanced H 2 production from corn stalk by integrating dark fermentation and single chamber microbial electrolysis cells with double anode arrangement. Int. J. Hydrogen Energy. 39, 8977-8982.

19. Liu, H., Cheng, S., Logan, B.E. 2005a. Production of electricity from acetate or

butyrate using a single-chamber microbial fuel cell. Environ. Sci. Technol. 39, 658-662.

20. Liu, H., Grot, S., Logan, B.E. 2005b. Electrochemically assisted microbial production of hydrogen from acetate. Environ Sci. Technol. 39, 4317-4320.

21. Logan, B.E., Call, D., Cheng, S., Hamelers, H.V., Sleutels, T.H., Jeremiasse, A.W., Rozendal, R.A. 2008. Microbial electrolysis cells for high yield hydrogen gas production from organic matter. Environ. Sci. Technol. 42, 8630-8640.

22. Logan, B.E., Hamelers, B., Rozendal, R., Schröder, U., Keller, J., Freguia, S., Aelterman, P., Verstraete, W., Rabaey, K. 2006. Microbial fuel cells: methodology and technology. Environ. Sci. Technol. 40, 5181-5192.

23. Lu, L., Xing, D., Ren, N., Logan, B.E. 2012. Syntrophic interactions drive the hydrogen production from glucose at low temperature in microbial electrolysis cells. Bioresour. Technol. 124, 68-76.

24. Montpart, N., Rago, L., Baeza, J.A., Guisasola, A. 2015. Hydrogen production in single chamber microbial electrolysis cells with different complex substrates. Water Res. 68, 601-615.

25. Nam, J.-Y., Yates, M.D., Zaybak, Z., Logan, B.E. 2014. Examination of protein degradation in continuous flow, microbial electrolysis cells treating fermentation wastewater. Bioresour. Technol. 171, 182-186.

26. Oh, S., Logan, B.E. 2005. Hydrogen and electricity production from a food processing wastewater using fermentation and microbial fuel cell technologies. Water Res. 39, 4673-4682.

27. Rader, G.K., Logan, B.E. 2010. Multi-electrode continuous flow microbial electrolysis cell for biogas production from acetate. Int. J. Hydrogen Energy. 35, 8848-8854.

28. Rozendal, R.A., Hamelers, H.V., Euverink, G.J., Metz, S.J., Buisman, C.J. 2006. Principle and perspectives of hydrogen production through biocatalyzed electrolysis. Int. J. Hydrogen Energy. 31, 1632-1640.

29. Rozendal, R.A., Hamelers, H.V., Molenkamp, R.J., Buisman, C.J. 2007. Performance of single chamber biocatalyzed electrolysis with different types of ion exchange membranes. Water Res. 41, 1984-1994.

30. Selembo, P.A., Perez, J.M., Lloyd, W.A., Logan, B.E. 2009. High hydrogen production from glycerol or glucose by electrohydrogenesis using microbial electrolysis cells. Int. J. Hydrogen Energy. 34, 5373-5381.

31. Sun, M., Mu, Z.-X., Sheng, G.-P., Shen, N., Tong, Z.-H., Wang, H.-L., Yu, H.-Q. 2010. Hydrogen production from propionate in a biocatalyzed system with in-situ utilization of the electricity generated from a microbial fuel cell. Int. Biodeter. Biodegr. 64, 378-382.

32. Tartakovsky, B., Manuel, M.-F., Wang, H., Guiot, S. 2009. High rate membrane-less microbial electrolysis cell for continuous hydrogen production. Int. J. Hydrogen Energy. 34, 672-677.

33. Tenca, A., Cusick, R.D., Schievano, A., Oberti, R., Logan, B.E. 2013. Evaluation of low cost cathode materials for treatment of industrial and food processing wastewater using microbial electrolysis cells. Int. J. Hydrogen Energy. 38, 1859-1865.

34. Torres, C.I., Marcus, A.K., Lee, H.-S., Parameswaran, P., Krajmalnik-Brown, R., Rittmann, B.E. 2010. A kinetic perspective on extracellular electron transfer by anode-respiring bacteria. FEMS Microbiol. Rev. 34, 3-17.

35. Torres, C.I., Marcus, A.K., Rittmann, B.E. 2007. Kinetics of consumption of fermentation products by anode-respiring bacteria. Appl. Microbiol. Biotechnol. 77, 689-697.

Chapter 4

Conclusions and Recommendations

4.1 Conclusions

The main goals of this study are to further utilize dark fermentation effluent in MECs, and to assess the impact of VFAs on MEC performance.

In this research, a comprehensive comparison of the effects of acetate, butyrate, and propionate on MEC is undertaken. For the first time the relationship between attached biomass and suspended biomass for butyrate and propionate in MEC has been established. Moreover, a literature review on continuous-flow operating MECs is also discussed in this thesis, to better understand the challenges associated with scale-up of MEC system.

The following conclusions can be drawn, based on the experimental findings of this study:

- The cycles fed with acetate had the highest peak of current density (6.0 ± 0.28 A/m^2), followed by the butyrate fed cycles (2.5 ± 0.06 A/m^2), and propionate fed cycles achieved the lowest current density (1.6 ± 0.14 A/m^2).

- The utilization rate of the substrates for ARB in MECs followed the order: acetate > butyrate > propionate.

- The cathodic hydrogen recovery decreased in the order of feeding with acetate, butyrate and propionate were 98 ± 0.8, 79 ± 4.9, and 71 ± 7.2 %, respectively.

- The coulombic efficiencies for acetate, butyrate, and propionate were 87 ± 5.7, 72 ± 2.0 and 51 ± 6.4 %.

- The SCOD removal efficiencies for butyrate and propionate were 88 ± 5.3 and 87 ± 5.8 % respectively.

- The calculated suspended biomass yield and the estimated attached biomass in the acetate-fed MEC were 0.042 g biomass COD/g substrate COD and 0.166 g biomass COD/g substrate COD, respectively.

- The calculated suspended biomass yield and the estimated attached biomass in the butyrate-fed MEC were 0.092 g biomass COD/g substrate COD and 0.341 g biomass COD/g substrate COD, respectively.

- The calculated suspended biomass yield and the estimated attached biomass in the propionate-fed MEC were 0.140 g biomass COD/g substrate COD and 0.510 g biomass COD/g substrate COD, respectively.

- Normalizing the maximum current density to the observed attached biomass yields 43.8, 20.1 and 8.7 A/mg biomass COD/m^2 for the acetate-fed, butyrate-fed, and propionate-fed cycles.

4.2 Recommendations

Even though further utilization of fermentation effluent in MEC to achieve higher hydrogen production is very promising, to scale-up from laboratory MECs to pilot-scale still needs a lot of work. The greatest challenge of scaling up MEC systems is that the hydrogen production rate is not high at low power input. Major advances in MEC configuration, the use of high-efficiency materials for electrodes and membranes, and efficient ARB having rapid substrate-utilization kinetics are required to achieve the goals of high hydrogen production rate and low applied voltage. Based on the findings of this study, further research should include:

- The configuration of the MEC could be modified. A membrane-less MEC could be studied. If the membrane-less MEC is applied, the method to inhibit the activities of methanogens should be emphasized.

- Anode potential could be controlled during the start-up period to culture a highly efficient ARB consortium.

- In this experiment, the anode respiring bacteria is cultivated from waste activated sludge. In the future, a combination of fermentation bacteria and anode respiring bacteria in MECs could be studied to learn whether glucose or complex carbohydrates could be degraded more efficiently in MEC or not.

- The MECs could be run in continuous-flow mode to facilitate scale-up in the future.

Appendices

These appendices consist of the following information:

The company of the materials, the MEC fabrication procedure, the pretreatment method of the materials, and the medium preparation used in this study are listed in Appendix A. The detailed calculation is shown in Appendix B.

Appendix A

A.1 Material summary

Table A1. 1 Materials summary

Items	Catalogue number	Supplier
Membrane	AMI-7001 Anion exchange membrane (AMI-7001S) (1.2m×0.5m sheet)	**Membrane International Inc**. 219 Margaret King Avenue, Ringwood, NJ 07456 USA Phone: 973-998-5530 / Fax: 973-998-5529 Email: customerservice@membranesinternational.com Website: http://www.membranesinternational.com
Anode (Carbon fiber)	24K Carbon Tow (100yd Roll)(Item # 2293-B)	**Fibre Glast Development Corp.** 385 Carr Drive Brookville, OH 45309 Phone: 800-838-8984 Fax: 937-833-6555 Email: customerservice@fibreglast.com Website: http://www.fibreglast.com
Cathode (stainless steel mesh)	Corrosion-Resistant Type 304 Stainless Steel Wire Cloth (mesh 50x50 and 12x12 in)	**McMaster Carr** 200 Aurora Industrial Pkwy. Aurora, OH 44202-8087 E-Mail: cle.sales@mcmaster.com Phone: 330-995-5500 Fax: (330) 995-9600 Website: http://www.mcmaster.com
Reference Electrodes	MF-2052 (RE-5B Ag/AgCl Reference Electrode with Flexible Connector)	**BASi** Purdue Research Park 2701 Kent Avenue West Lafayette, IN 47906 USA 800.845.4246 Fax 765.497.1102 Website: http://www.basinc.com/products/ec/ref.php

A.2 MEC fabrication

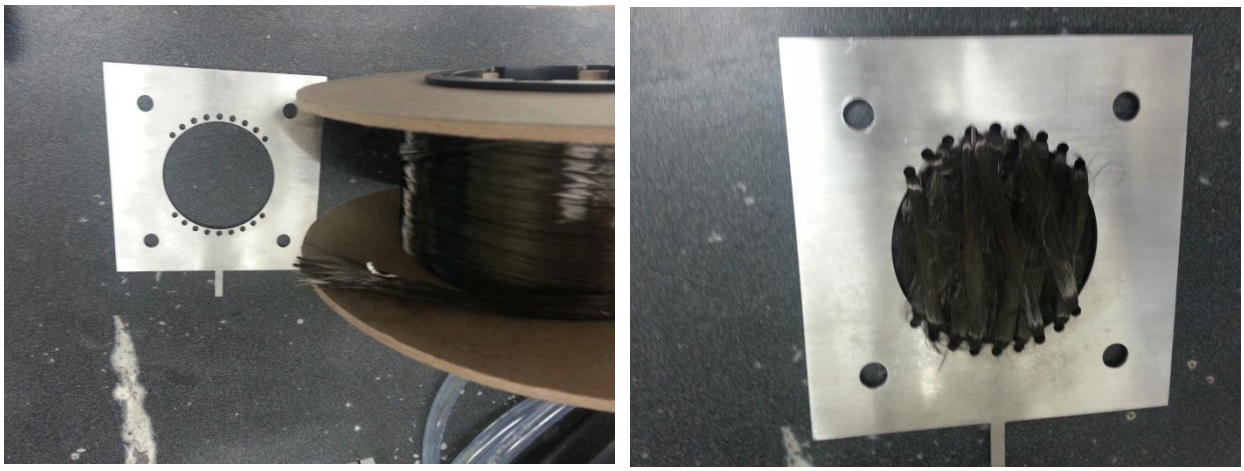

Figure A2.1 -- Anode preparation: materials used for anode (left) and wrapping around the anode electrode with carbon fiber (right).

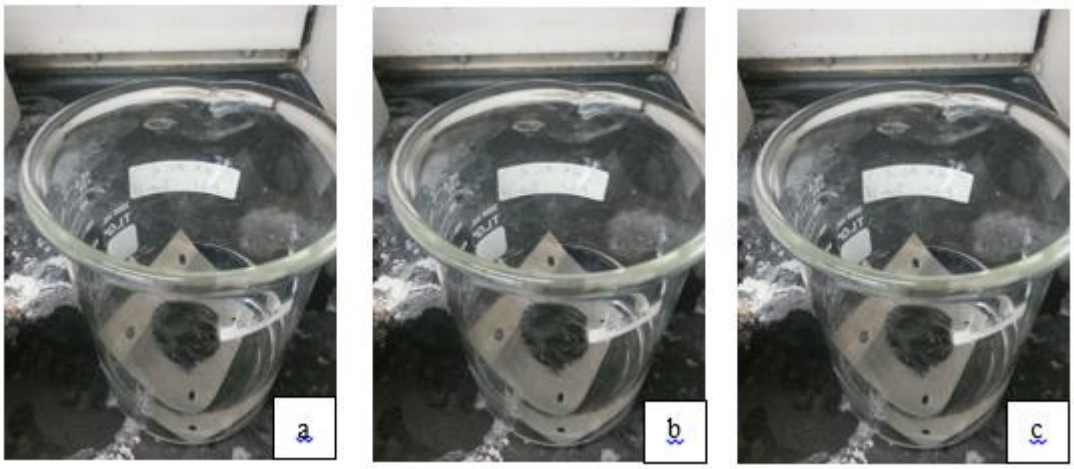

Figure A2.2 -- Pretreatment of the anode in the fume hood: a) 1st day with nitric acid (1N); b) 2nd day with acetone (1N); c) 3rd day with ethanol (1N)

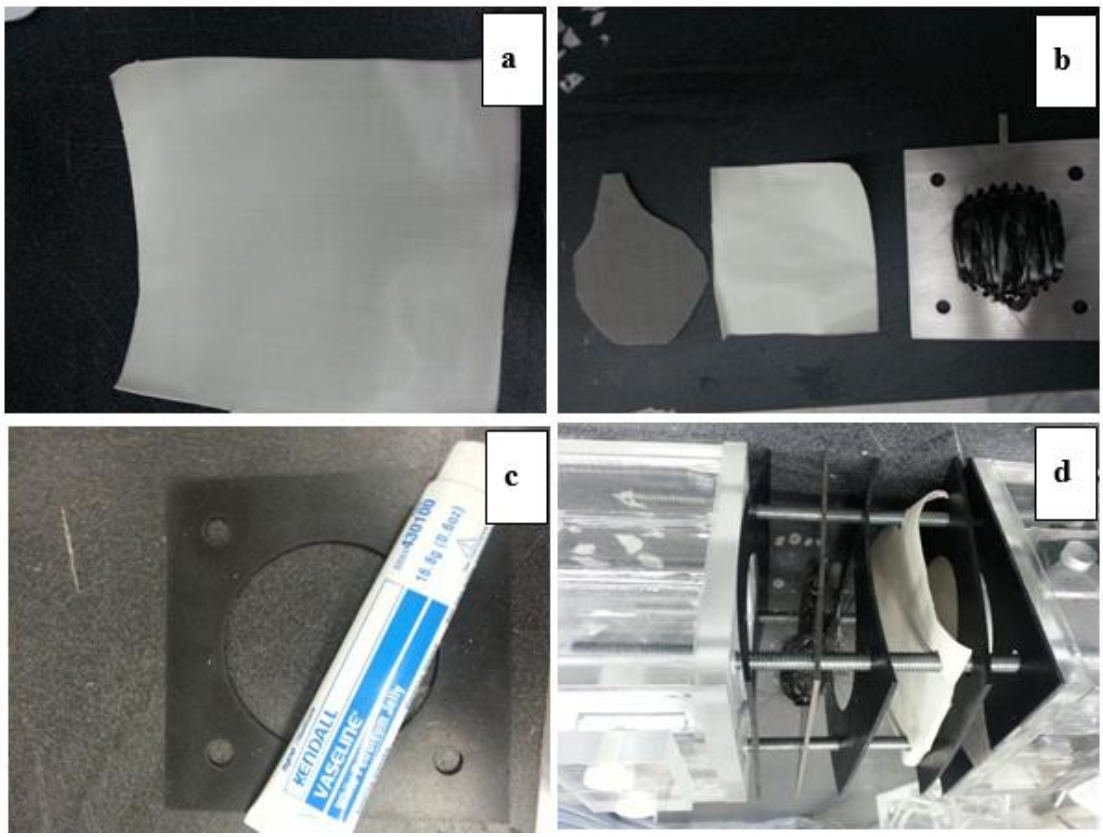

Figure A2.3 -- (a) Membrane after pretreatment: 24 hours at 40^{o}C in 5% NaCl solution (b) Cathode (left), membrane (middle) and anode (right) (c) Brushing Vaseline onto rubber to prevent leaking (d) Connecting the anode chamber, anode electrode, membrane, cathode electrode and cathode chamber together

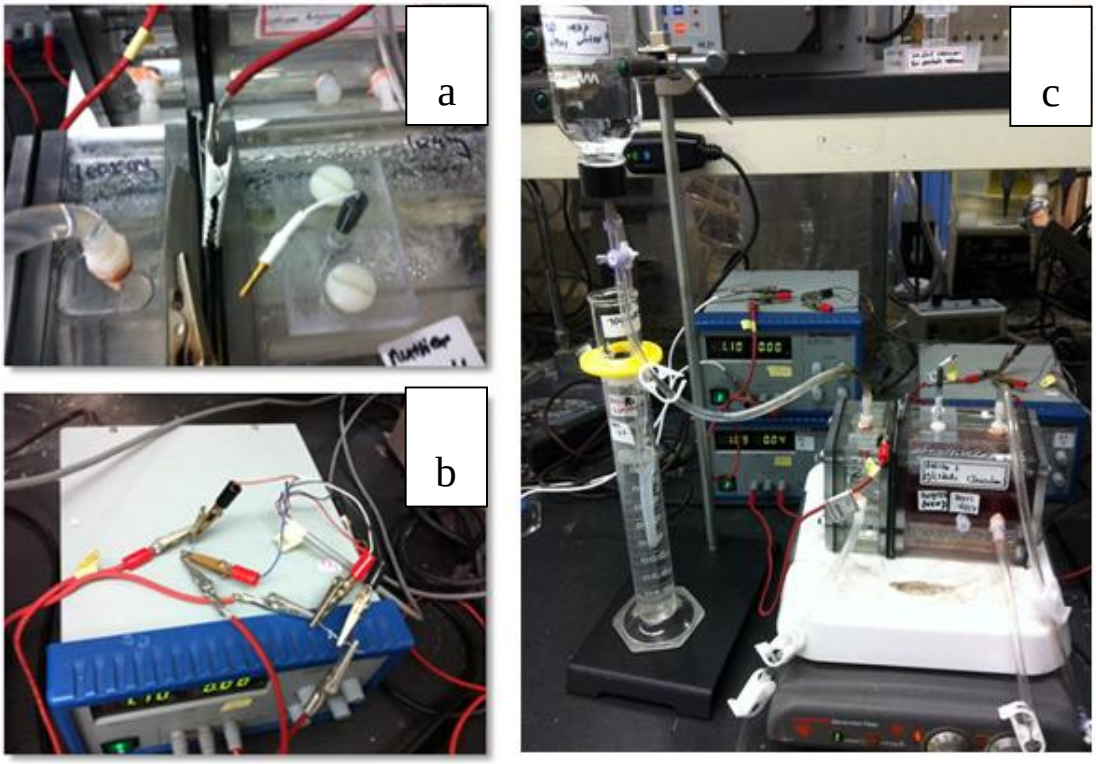

Figure A2.4 – (a) Picture of connecting the anode and cathode electrode to the power supply (b) A resister is connected in series with anode and cathode (c) Set-up picture of the MEC system

A.3 Pretreatment method

A3.1 Carbon fiber pretreatment (3 days in series)

- 1st day with nitric acid (1N)
- 2nd day with acetone (1N)
- 3rd day with ethanol (1N)

Table A3.1 -- The summary of the solution preparation

Time (d)	Solution		Solution (mL)	Water (mL)
1	nitric acid	HNO_3	50.96	749.04
2	acetone	$(CH_3)_2CO$	58.87	741.13
3	ethanol	C_2H_6O	46.71	753.29

Normality of a solution = Molarity × the number of equivalents per moles
For example, 1M H_2SO_4 = 2N H_2SO_4

- HNO_3 in the lab

Density (ρ) = 1.413 g/mL = 1.413kg/L
Formula Weight (FW) = 63.01 g/mol
70 wt. % = 70 grams of HNO_3/100 grams of this acid

In order to immerge all the material, at least800mL totally solution is needed.

1N HNO_3 = 1M HNO_3 = 1mol/L HNO_3
Assume V (L) of the nitric acid solution is needed to add to (0.8-V) L water

$$\frac{\rho \times V \times 70\%}{FW \times 0.8L} = 1\ mol/L$$

$$\frac{\frac{1.413kg}{L} \times V \times 70\%}{63.01g/mol \times 0.8L} \times \frac{1000g}{kg} = 1\ mol/L$$

V= 0.05096L =50.96mL HNO_3 solution
V'= 800-50.96 = 749.04 mL water
So that adding 50.96mL HNO_3 to 749.04mL water.

- Acetone $(CH_3)_2CO$ in the lab

Density (ρ) = 0.79 g/mL = 0.79 kg/L
Formula Weight (FW) = 58.08 g/mol

99.9 %
In order to immerge all the material, at least800mL totally solution is needed.

1N $(CH_3)_2CO$ = 1M $(CH_3)_2CO$ = 1mol/L $(CH_3)_2CO$
Assume V (L) of the acetone solution is needed to add to (0.8-V)L water

$$\frac{\rho \times V \times 99.9\%}{FW \times 0.8L} = 1\ mol/L$$

$$\frac{\frac{0.79kg}{L} \times V \times 99.9\%}{58.08g/mol \times 0.8L} \times \frac{1000g}{kg} = 1\ mol/L$$

V= 0.05887L =58.87mL Acetone solution
V'= 800-58.87 = 741.13mL water
So that adding 58.87mL Acetone to 741.13mL water.

- Ethanol C_2H_6O

Density (ρ) = 0.789 g/mL = 0.789 kg/L
Formula Weight (FW) = 46.07 g/mol
100%

$$\mathrm{V} = \frac{\frac{1mol}{L} \times \frac{46.07g}{mol} \times 0.8L}{100\% \times \frac{0.789kg}{L} \times 1000g/kg} = 0.0467L = 46.71mL$$

V'= 800-46.71 = 753.29mL water
So that adding 46.71 mL Ethanol to 753.29mL water.

A3.2. Membrane pre-treatment

24 hours at 40 ℃ in 5% NaCl solution (5 g NaCl/100 mL water)

$$\mathrm{V}_{water} = \frac{100g}{1000kg/m^3} \times \frac{kg}{1000g} \times \frac{1000L}{m^3} = 0.1L = 100mL$$

A.4 Medium preparation

Table A3.1 -- Chemicals for macro medium preparation

1L of medium							
Macro (adding the chemicals into 1L water)							
Chemicals		MWT g/mol	needed g	needed mM	reality g	reality mM	error %
Potassium Phosphate Monobasic	KH_2PO_4	136.09	2.3	16.90			
Sodium Phosphate, Dibasic, 7 Hydrate	Na_2HPO_4-$7H_2O$	268.07	8.8	32.83			
Ammonium chloride	NH_4Cl	53.49	0.038	0.71			
Sodium bicarbonate	$NaHCO_3$	84.01	0.84	10.00			

Table A3.2 -- Chemicals for micro medium preparation

Micro (adding the chemicals into 1L water)							
Chemicals		MWT g/mol	needed g	needed mM	Reality g	reality mM	Error %
Magnesium chloride	$MgCl_2$-$6H_2O$	203.3	0.025	0.1230			
Manganese chloride tetrahydrate	$MnCl_2$-$4H_2O$	197.91	0.006	0.0303			
Calcium chloride dihydrate	$CaCl_2$-$2H_2O$	147.01	0.0012	0.0082			
Zinc chloride	$ZnCl_2$	136.3	0.0005	0.0037			
Nickel (II) chloride	$NiCl_2$	129.6	0.00011	0.0008			
Cupric sulfate pentahydrate	$CuSO_4$-$5H_2O$	249.69	0.0001	0.0004			
Aluminum potassium sulfate dodecahydrate	$AlK(SO_4)_2$-$12H_2O$	474.39	0.0001	0.0002			
Cobalt (II) Nitrate Hexahydrate	$Co(NO_3)_2$-$6H_2O$	291.03	0.001	0.0034			
Boric acid	H_3BO_3	61.83	0.0001	0.0016			
Ethylenedoaminetetraacetic acid	EDTA ($C_{10}H_{16}N_2O_8$)	292.24	0.005	0.0171			
Sodium Tungstate -2- Hydrate Pure	Na_2WO_4-$2H_2O$	329.85	0.0001	0.0003			
Sodium Hydrogen Selenite	$NaHSeO_3$	150.96	0.0001	0.0007			
Sodium molybdate dihydrate	Na_2MoO_4-$2H_2O$	241.95	0.0002	0.0008			

Table A3.3 -- 77mM Na_2S-$9H_2O$ preparation

Adding Na_2S-$9H_2O$ into 500mL water							
Chemicals		MWT g/mol	needed g	needed mM	Reality g	reality mM	error %
Sodium sulfide nonahydrate	Na_2S-$9H_2O$	240.18	9.24693	77			

Table A3.4 -- 20mM $FeCl_2$-$4H_2O$ preparation

Adding $FeCl_2$-$4H_2O$ into 500mL water							
Chemicals		MWT g/mol	needed g	needed mM	reality g	reality mM	error %
Ferrous chloride tetrahydrate	$FeCl_2$-$4H_2O$	198.81	1.9881	20			

Appendix B. Calculation summary

1. Anode specific surface area of the fibers

Fiber's diameter = 7 μm
Fiber's length = 150 cm
The fiber bundle contained 24000 individual carbon filaments.

The geometric surface of the fibers is

$$= 7\mu m \times 3.14 \times 150cm \times 24000 \times \frac{cm}{10000\mu m} = 7912.8\ cm^2$$

The volume of the fibers is

$$= (\frac{7\mu m}{2})^2 \times 3.14 \times 150cm \times 24000 \times \left(\frac{cm}{10000\mu m}\right)^2$$
$$= 1.38474\ cm^3$$

The specific surface area of the fibers is

$$= \frac{7912.8cm^2}{1.38474\ cm^3} \times \frac{m^2}{10000cm^2} \times \frac{1000000cm^3}{m^3} = 571429\ \frac{m^2}{m^3}$$

2. Hydrogen production rate in reality

$$\text{Total Volume of gas (mL)} = \text{Water being replaced(mL)}$$
$$\text{Percentage of hydrogen} \rightarrow \text{From GC}$$
$$\text{Hydrogen Volume (mL)} = \text{Total Volume of gas(mL)} \times \text{Percentage of hydrogen(\%)}$$

$$PV = nRT$$
$$n(H_2) = \frac{PV}{RT}$$

Assume: Room Temperature 25℃=298K, R=0.08206 (L·atm)/(mol·K), P=1atm

$$n(H_2)\text{ production in reality (mol)} = \frac{PV}{RT}$$
$$= \frac{1atm \times \text{Hydrogen Volume(mL)}}{0.08206\ (L \cdot atm)/(mol \cdot K) \times 298K} \times \frac{L}{1000mL}$$
$$= 0.0000408933 \cdot \text{ Hydrogen Volume}$$

3. Hydrogen production rate in reality

$$\text{Hydrogen Production Rate in Reality } (\frac{\text{m}^3\text{H}_2}{\text{m}^3\text{Anode day}})$$

$$= \frac{\text{V}(\text{H}_2) \text{ production in reality}}{\text{Anode Volume } \cdot \text{d}}$$

$$\text{Hydrogen Production Rate in Reality } (\frac{\text{m}^3\text{H}_2}{\text{m}^2\text{Anode day}})$$

$$= \frac{\text{V}(\text{H}_2) \text{ production in reality}}{\text{Anode Surface Area } \cdot \text{d}}$$

4. Transfer H_2 production to volume

Assume: Room Temperature 25℃=298K, R=0.08206 (L·atm)/(mol·K), P=1atm

$$\text{V}(H_2)\ production\ in\ theory\ (L) = \frac{nRT}{P}$$

$$= \frac{0.08206 \frac{L \cdot atm}{mol \cdot K} \times 298K \times \text{n}(H_2) \left(\frac{mol}{d}\right)}{1atm} = 24.45388 \cdot\ n(H2)$$

5. Hydrogen production rate in theory

From the COD reduction, we can get how much Acetate consumed.

$$C_2H_4O_2 + 2O_2 = 2H_2O + 2CO_2$$

$$\text{n(HAc)}(\frac{mol}{d}) = \frac{\Delta SCOD(\frac{mg}{d})}{2 \times 32g/mol} \times \frac{g}{1000mg} = 0.000015625 \cdot \Delta SCOD$$

From Acetate consumed rate, we can get the hydrogen producing rate.

$$C_2H_4O_2 + 2H_2O = 4H_2 + 2CO_2$$

$$\text{n}(H_2)(\frac{mol}{d}) = 4 \times \text{n(HAc)} = 0.0000625 \cdot \Delta SCOD$$

6. Hydrogen yield

$$\text{H}_2 \text{ Yield } \left(\frac{\text{mol H}_2}{\text{mol HAc}}\right) = \frac{\text{H}_2 \text{ Production in reality (mol)}}{\text{HAc consumed during this time interval (mol)}}$$

$$\mathrm{H_2\ Yield}\left(\frac{\mathrm{L\ H_2}}{\mathrm{g\ SCOD}}\right) = \frac{\mathrm{H_2\ Production\ in\ reality\ (mL)}}{\mathrm{SCOD\ removed\ during\ this\ time\ interval\ (mg)}}$$

$$\mathrm{H_2\ Yield}\left(\frac{\mathrm{L\ H_2}}{\mathrm{g\ HAc}}\right) = \frac{\mathrm{H_2\ Production\ in\ reality\ (mL)}}{\mathrm{HAc\ consumed\ during\ this\ time\ interval\ (mg)}}$$
$$= \frac{\mathrm{H_2\ Production\ in\ reality\ (mL)}}{\mathrm{HAc\ consumed\ during\ this\ time\ interval\ (mol)} \times 60\mathrm{g/mol}}$$
$$\times \frac{\mathrm{L}}{1000\mathrm{mL}}$$

7. Coulombic efficiency

$$Coulombic\ Efficiency = \frac{Coulombs\ Recovered\ as\ current}{Total\ Coulombs\ in\ substrate}$$

$$Coulombs\ Recovered\ as\ current\ (mol) = \frac{\int_0^t I\ t}{2F}$$

Where I is the current (A, C/s)
t is the time interval (s)
2 is used to convert moles of electrons to moles of hydrogen
F is the Farady constant (96485 C/mol e-)

8. Energy efficiency

$$\mathrm{Energy\ Input} = \mathrm{IEps} - \mathrm{IR_{ex}}^2$$
$$\mathrm{R_{ex}} = 10\Omega$$
$$\mathrm{Eps} = 1\mathrm{V}$$

$$\mathrm{Energy\ Recovered\ as\ Hydrogen} = \Delta\mathrm{H} \times \mathrm{n(H2)in\ reality}$$
$$\Delta\mathrm{H} = 285.83\mathrm{KJ/mol}$$

$$\mathrm{Energy\ Efficiency} = \frac{\mathrm{Energy\ Input}}{\mathrm{Energy\ Recovered\ as\ Hydrogen}}$$

9. Substrate concentration

The acetate corresponding COD is 1600 mg/L, in order to calculate how much

of sodium acetate should be prepared, the following calculations are used.

$$CH_3COOH + 2O_2 = 2CO_2 + 2H_2O$$

$$TCOD = 2 \times \frac{32\ g}{mol} \times c(CH_3COOH) = 1.6\ mg/L$$

$$c(CH_3COOH) = \frac{1.6\ g/L}{2 \times 32} = 0.025 mol/L$$

$$c(CH_3COONa) = \frac{0.025\ mol}{L} \times \frac{82g}{mol} = 2.05\ g/L$$

The propionate and butyrate are also prepared in the same way. Instead of 1600 mg/L initial COD, 800 mg/L initial COD is used for propionate and butyrate. The substrates were prepared from sodium propionate and sodium butyrate.

$$C_2H_5COOH + 3.5O_2 = 3CO_2 + 3H_2O$$

$$TCOD = 3.5 \times \frac{32\ g}{mol} \times c(CH_3COOH) = 0.8 g/L$$

$$c(C_2H_5COOH) = \frac{0.8\ g/L}{3.5 \times 32} = 0.00714\ mol/L$$

$$m(C_2H_5COONa) = \frac{0.00714\ mol}{L} \times \frac{96g}{mol} = 0.686\ g/L$$

$$C_3H_7COOH + 5O_2 = 4CO_2 + 4H_2O$$

$$TCOD = 5 \times \frac{32\ g}{mol} \times c(CH_3COOH) = 0.8 g/L$$

$$c(C_2H_5COOH) = \frac{0.8\ g/L}{5 \times 32} = 0.005 mol/L$$

$$m(C_2H_5COONa) = \frac{0.005\ mol}{L} \times \frac{110g}{mol} = 0.55\ g/L$$

Table B.1 -- Summary of the substrate preparation

Chemicals	Molecular weight (g/mol)	Concentration (g/L)	Corresponding COD (mg/L)

Sodium Acetate (CH_3COONa)	82	2.05	1600
Sodium Propionate (C_2H_5COONa)	96	0.686	800
Sodium Butyrate (C_3H_7COONa)	110	0.55	800
Glucose ($C_6H_{12}O_6$)	180	1.5	1600

Curriculum Vitae

Name: Nan Yang

Post-secondary Education and Degrees:

Western University
London, Ontario, Canada
Master of Engineering Science
2013 – Present

Western University
London, Ontario, Canada
Master of Engineering
2012 – 2013

Dalian University of Technology
Dalian, Liaoning, China
Bachelor of Engineering
2008 – 2012

Honors and Awards:

Fully funded Masters' tuition recipient
2013 – 2015

Related Work Experience

Internship
TrojanUV technology
2015 – Present

Teaching Assistant
Western University
2014 – 2015

Publications

Yang N., Hafez H., Nakhla G., (2015). Impact of Volatile Fatty Acids on Microbial Electrolysis Cell Performance. Bioresour Technol.